Summer 8-7-2012

Lake Cycles and Sediments: Locality 80, Olduvai Gorge, Tanzania

Patricia A. Berry
Georgia State University

LAKE CYCLES AND SEDIMENTS:

LOCALITY 80, OLDUVAI GORGE, TANZANIA

by

PATRICIA ANNE BERRY

Under the Direction of Daniel Michael Deocampo

ABSTRACT

Studies have shown that Bed I and Lower Bed II (1.92Ma- 1.76Ma) of Paleolake Olduvai at Locality 80 are primarily composed of the authigenic lacustrine clay minerals illite, smectite, and interlayered illite-smectite. X-ray fluorescence analysis and the sedimentation rates of Hay and Kyser (2001) were used to identify four apparent lake cycles beginning and ending with saline alkaline phases. Peaks in Al_2O_3/MgO ratios, and TiO_2 and P_2O_5 abundances occur at approximately the same elevations within the stratigraphic section. Low values in these three parameters indicate saline alkaline conditions whereas high values represent fresh water conditions. Lake Cycles (LC) 1 and 4 completed in approximately 44,000 years and 42,000 years respectively, which is similar to the 41k.y. year cycle associated with Earth's obliquity. Lake Cycles 2 and 3 span approximately 24,000 years and are similar to the 21k.y. precession cycle.

INDEX WORDS: Clay minerals, Environmental proxy, Lacustrine sediments, Olduvai Gorge, Paleoclimate, Saline alkaline lake

LAKE CYCLES AND SEDIMENTS:

LOCALITY 80, OLDUVAI GORGE, TANZANIA

by

PATRICIA ANNE BERRY

A Thesis Submitted in Partial Fulfillment of the Requirements for the Degree of

Master of Science

in the College of Arts and Sciences

Georgia State University

2012

LAKE CYCLES AND SEDIMENTS:

LOCALITY 80, OLDUVAI GORGE, TANZANIA

by

PATRICIA ANNE BERRY

Committee Chair: Daniel Michael Deocampo

Committee: W. Crawford Elliott

Lawrence M. Kiage

Electronic Version Approved:

Office of Graduate Studies

College of Arts and Sciences

Georgia State University

July 2012

ACKNOWLEDGEMENTS

I would like to thank the following people:

Dr. Gail Ashley, Rutgers, The State University of New Jersey, for her guidance and wisdom.

Dr. Daniel Deocampo, for questioning my ability to actually complete my thesis while working full time and caring for five children, it only made me that much more determined to finish it!

Dr. Crawford Elliott, for serving on my committee and providing support.

Dr. Lawrence Kiage, for serving on my committee and providing thoughtful insights.

The Department of Geosciences at Georgia State University, for providing the equipment and instruction that made this all possible.

Kimberly Sams, for her mad formatting skills and moral support.

Southern States Energy Board, for a flexible work schedule, I finished my thesis and I still have a job!

My husband, Nick Marroni, for countless hours grinding rocks into powder and for telling me that he would be disappointed in me, when I wanted to give up.

My mom, Pam Berry, for babysitting – "*When are you going to pick them up?*"

My children, for being patient while mommy spent many nights and weekends on the computer, Hailey, Josh, Lily, Nathan and Abbey – "*Thesis is a bad word!*"

TABLE OF CONTENTS

LIST OF TABLES

LIST OF FIGURES

LIST OF ABBREVIATIONS

Al	Aluminum
Al_2O_3	Aluminum Oxide
Avg	Average
CB	Central Basin
ELM	Eastern Lake Margin
I/S	Illite-Smectite
K	Potassium
K_2O	Potassium Oxide
LC	Lake Cycle
Loc 80	Locality 80
LOI_x	Loss on Ignition x=temperature
Mg	Magnesium
MgO	Magnesium Oxide
P_2O_5	Phosphorus
R^2	Correlation coefficient
Sed	Sediment
USGS	United States Geological Survey
WLM	Western Lake Margin
XRD	X-ray Diffraction
XRF	X-ray Fluorescence

1. INTRODUCTION

Paleoanthropological discoveries in Olduvai Gorge and the possible correlations between African climate change and biological evolution have created the demand for high resolution paleoclimate records (Leakey, 1971; deMenocal, 1995; Liutkus et al., 2005). Clay minerals, like those present in the lacustrine sediments at Paleolake Olduvai, are sensitive to both weathering in the drainage basin and the chemical composition of the lake water (Singer and Stoffers, 1980; Hay and Kyser, 2001; Yuretich et al., 2002; Deocampo, 2004; Deocampo et al., 2010). These clay-rich sediments act as chemical sinks for a variety of lacustrine ions and can provide geochemical records of earth and ecosystem history that are both highly resolved in time and of long duration (Yuretich and Cerling, 1983; Yuretich et al., 1995; Hay and Kyser, 1996; Deocampo et al., 2000; Cohen, 2003). Due to its small size and thus likelihood to be highly responsive to climate change, Paleolake Olduvai is an ideal location in which to examine the East African paleoclimate (Singer and Stoffers, 1980; Hay and Kyser, 2001; Yuretich et al., 2002).

The goal of this study is to reconstruct the wet/dry lake cycles of Paleolake Olduvai that occurred between 1.92 and 1.76 Myr. This period of time is of particular interest because the earliest members of the genus *Homo* occur in East African sediments around 1.9Myr; *Homo erectus* first appears near 1.8Myr and by 1.6Myr *Homo habilis* becomes extinct (deMenocal, 1995). X-ray Fluorescence (XRF) Spectroscopy was used to measure select major and trace elements from the detrital and authigenic lacustrine sediments present at Locality 80 (Loc 80), Olduvai, Gorge Tanzania. As the majority of the sediments at Loc 80 are illite, smectite, and I/S, an emphasis is placed on the relationships between the following oxides and their ratios, Al_2O_3/MgO, TiO_2, and P_2O_5.

1.1 Plio-Pleistocene East African Paleoclimate

Marine paleoclimate records demonstrate a Plio-Pleistocene African climate that is characterized by alternating wet and dry conditions (deMenocal, 1995; Levin et al., 2004; Trauth et al.,

2009). The intensity of the African monsoon has been influenced by periodic variations in low latitude insolation (solar radiation energy), resulting from both Earth's orbital precession (direction of the Earth's axis of rotation) and to a lesser extent obliquity (axial tilt) (deMenocal, 1995; Tuenter et al., 2003; Ashley, 2007). According to Tuenter et al (2003) monsoonal precipitation is enhanced during either maximum obliquity or minimum precession. Additionally summer season insolation, which drives monsoonal circulation, increased when perihelion (minimum Earth-Sun distance with regard to orbit) coincided with boreal summer (summer in the northern hemisphere, relating to the north wind) (deMenocal, 1995; Levin et al., 2004; Trauth et al., 2009). Higher insolation leads to an enhanced temperature contrast between the land and sea (Tuenter et al., 2003). Heating of the land relative to the ocean causes a greater land-ocean pressure difference and leads to stronger monsoonal circulation and increased precipitation (Tuenter et al., 2003). African paleolake levels and tropical paleoriver outflow were greatest during the augmented summer season insolation and indicate increased monsoon intensity(deMenocal, 1995).

Additionally, Pleistocene lacustrine records from subtropical Africa indicate that the development of arid conditions was synchronous with high latitude cold events and that cold glacial North Atlantic sea-surface temperatures covary with glacial ice volume fluctuations (deMenocal, 1995). These fluctuations oscillate at high latitude between moderate glacial and interglacial extremes at the 41 k.y. orbital obliquity cycle which regulates high-latitude seasonal insolation (deMenocal, 1995).

1.2 Geologic / Geographic Setting

1.2.1 Location

Paleolake Olduvai is located at the center of the Olduvai Basin which lies on the western margin of the eastern branch of the East African Rift (a.k.a. Gregory Rift) in northern Tanzania. It falls between the Pliocene-Pleistocene Ngorongoro Volcanic Highland and the Serengeti Plain (Figure 1) (Ashley,

2007). The area of interest for this study is Locality 80 (2°57'89.0N, 35°18' 52.5E) (Loc 80)(Hay, 1976a). Loc 80 occurs west of the Fifth Fault in the central basin(CB), (Figure 2) (Hay and Kyser, 2001).

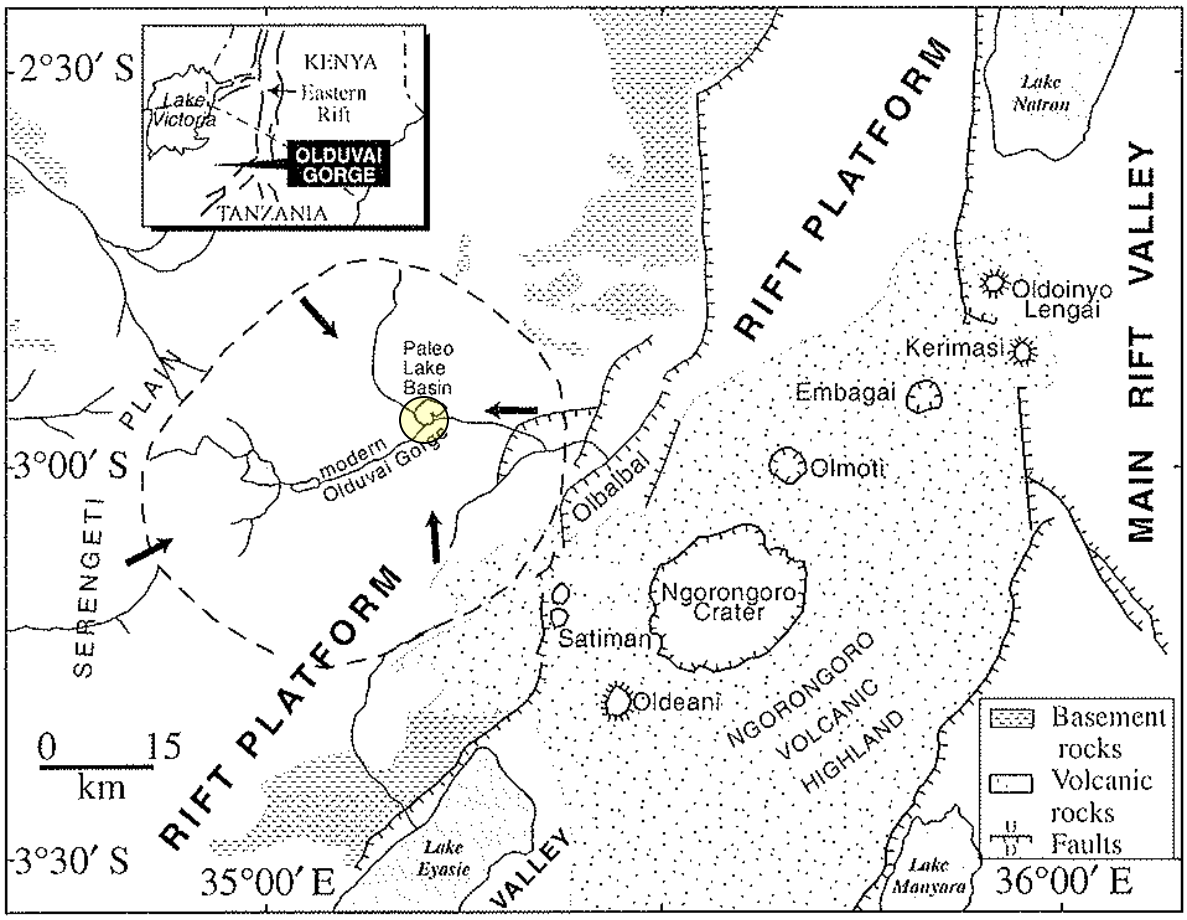

Figure 1 The General location of the main rift valley and rift platform at 3 degrees south.
The drainage pattern of the modern Olduvai Gorge and approximate position of the paleolake in the center of the basin is depicted. The approximate location of the paleobasin is indicated by a dashed line. (After (Ashley, 2007).

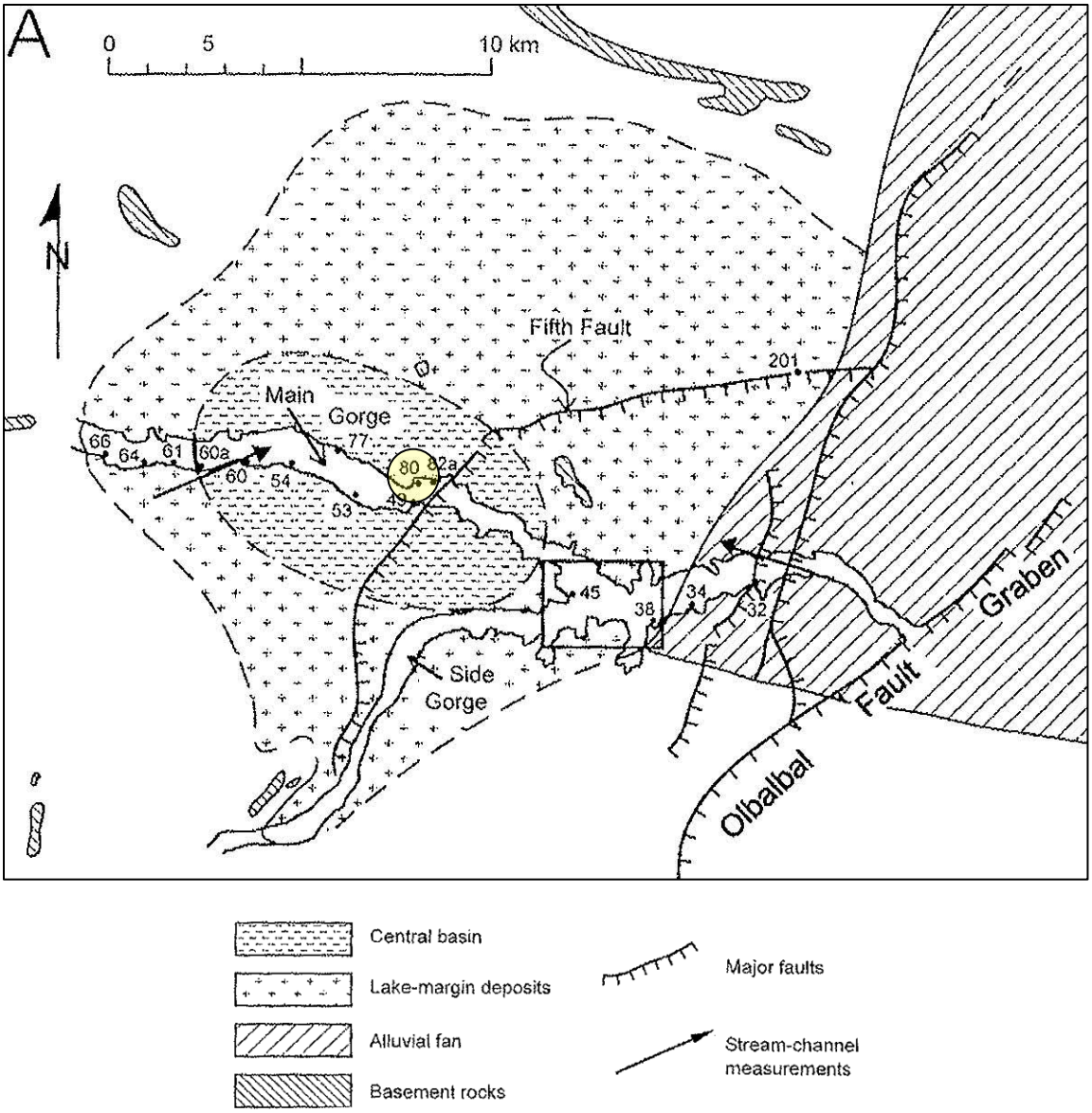

Figure 2 Inferred paleogeography of Paleolake Olduvai

Inferred paleogeography of Paleo Lake Olduvai in which the central basin is shown for the lowermost part in unit 3. Numbered localities are from Hay (1976). Outer limits of the central basin and lake margin zone are clearly established only where intersected by the gorge and at and near locality 201 (after (Hay and Kyser, 2001).

1.2.2 The Olduvai Beds

The Olduvai beds are divided into seven formations, Bed I, Bed II, Bed III, Bed IV, the Masek Beds, the Ndutu Beds and the Naisiusiu Beds (Hay, 1976b). The focus of this study is Bed I and Lower Bed II at Locality 80. Bed I is the lowermost mappable unit of the Olduvai Beds and occupies most of the Olduvai basin (Hay, 1976b). It is subdivided into five paleoenvironments based on lithologic interpretations: lake deposits, lake-margin deposits, alluvial fan deposits, alluvial-plain deposits and lava flows (Hay, 1976b; Hay, 1981). Loc 80 occurs within the Bed I lake deposits. The lake deposits in Bed I are comprised of eighty percent claystone, fifteen percent tuff, three percent limestone and dolomite, two percent sandstone and an additional fraction of chert and conglomerate (Hay, 1963; Hay, 1976b; Hay, 1981; Hay and Kyser, 2002). Bed I pinches out against the Naabi Ignimbrite to the west and is overlain by Tuff IF (Hay, 1976b; Hay, 1981).

Bed II occurs over a greater lateral extent than Bed I (Hay, 1963; Hay, 1967; Hay, 1976b). A widespread disconformity subdivides Bed II into two units of differing lithology and paleoenvironmental settings (Hay, 1976b). The deposits below the disconformity are referred to as Lower Bed II and have many features in common with Bed I (Hay, 1976b). Bed II deposits are interpreted as representing seven paleoenvironments: alluvial fan, alluvial plain, lake, lake margin, eolian and a lake stream complex (Hay, 1976b). Loc 80 occurs within the lake deposits of Lower Bed II. The lake deposits in Bed II below the lowermost disconformity and west of the Fifth Fault are comprised of seventy percent claystone, twenty-two percent tuff, five percent carbonate rocks, three percent sandstone and less than one percent of chert and conglomerate(Hay, 1976b; Hay and Kyser, 2002). Lower Bed II is defined by Tuff IF at the base and a disconformity at the top which separates it from the rest of Bed II.

The lower most disconformity that occurs in Bed II is likely the result of active tectonics (Hay, 1963, 1970; Hay, 1976b). During the deposition of Bed II a widespread episode of faulting began and had

effect on the entire Olduvai basin (Hay, 1976b). The deposits that occur above the disconformity include lake deposits, mixed fluvial-lacustrine deposits and fluvial deposits (Hay, 1976a).

1.2.3 Depositional History and Origin of Deposits

The Olduvai basin lies to the west of the major faults and volcanoes of the Eastern Rift Valley in Northern Tanzania (Hay, 1976b; Ashley and Hay, 2002). The basin is of extensional tectonic origin and was formed through the growth of the Ngorongoro volcanic highlands and extensive faulting (Hay, 1976b; Hay, 1981; Ashley and Hay, 2002). The Olduvai basin was tilted downward to the east during deposition of Bed I and faulting began early during the deposition of Bed II with the downward displacements tending to occur on the eastern side (Hay, 1976b; Hay and Kyser, 2001). Bed I and Lower Bed II were deposited between ca. 1.92 and 1.7 Ma (Hay and Kyser, 2001).

The Olduvai sediments were transported by fluvial and eolian processes and many were also modified by pedogenic activity (Hay, 1976b). There are multiple sediment types that occur within the Olduvai basin; pyroclastics, claystones, carbonates, sandstone: arkosic / lithic wacke and sandstone: quartzose / feldspathic wacke (Ashley and Hay, 2002). Claystone and tuff are the dominant sediments in the center of the paleolake at Loc 80.

The phyllosilicates montmorillonite (a member of the smectite family) and illite are both common sedimentary minerals (Hay, 1976b; Hay and Kyser, 2001; Ashley and Hay, 2002). These minerals may form through the weathering of volcanic rocks and the metamorphic micaceous basement rocks as well as the interaction of detrital clays with the saline alkaline water that was present in Paleolake Olduvai (Hay, 1970; Hay, 1976b; Hay and Kyser, 2001).

Carbonates are also present and occur as sand-sized euhedral calcite crystals and nodules as well as to a much lesser extent limestone and dolostone(Hay and Kyser, 2001; Ashley and Hay, 2002). The carbonates have been interpreted as the products of diagenetic alteration of gaylussite $Na_2Ca(CO_3)_2{\cdot}5H_2O$ (Deer et al., 1992; Hay and Kyser, 2001).

1.3 Paleolake Olduvai

The lake basin was hydrologically closed and can be subdivided into three zones: a central basin (CB) that contained a perennial saline lake; a surrounding eastern lake margin (ELM) zone that was flooded for extended periods by saline alkaline water and a western lake margin (WLM) zone which was flooded less frequently than the ELM (Figure 2) (Hay, 1976b; Hay and Kyser, 2001). The water of Paleolake Olduvai was shallow, saline and alkaline (Hay, 1976b; Hay, 1981; Hay and Kyser, 1996, 2001; Ashley and Hay, 2002). It episodically flooded, up to 15 km in diameter when fully expanded, as climatic variations controlled the balance between inflow and evaporation (Hay, 1976b; Hay, 1981; Hay and Kyser, 2001; Ashley and Hay, 2002).

1.3.1 Locality 80 Stratigraphy and Unit Subdivision (Based on Hay and Kyser 2001)

According to Hay and Kyser 2001 the Central Basin sequence is divided into four units of differing lithology representing different lacustrine paleoenvironments. Each subdivision is based on evidence of subaerial exposure and content of calcite crystal limestones. Additional diagnostic features are claystone color and evidence of former evaporites. In order to allow for a more accurate comparison the stratigraphic column at Loc 80 is based on the units described in Hay and Kyser (2001) (Figure 3). Photographs of the outcrop where the samples for this study were obtained are shown in Figure 4, Figure 5 and Figure 6. The locations of the samples, in this study, in relation to major stratigraphic markers can be found in Figure 11, Figure 12, and Figure 13.

Unit I is 10.1m thick and Tuff IA is the basal bed. The Unit is 80% claystone, 10% tuff and 10% dolostone. Claystones are typically massive and waxy with olive hues. Some sand size calcite crystals and dolomite are dispersed throughout the clay. There are no calcite-crystal limestones or evidences of subaerial exposure.

Unit 2 is 6.8m thick and Tuff IB forms the topmost layer. The unit largely consists of waxy claystone and resembles Unit 1. Calcite crystal limestones are common and range in thickness from a

few millimeters to 20cm. The limestones appear to be continuous and of uniform thickness. Surface exposure of the central area is indicated by desiccation cracks filled by calcite crystal.

Unit 3 is 5.9m thick and extends from the top of Tuff IB to the top of Tuff IF. The unit is 76% claystone, 22% tuff and 2% dolomite. The Claystones are less waxy and browner than those of Units 1 and 2. They are massive except for areas that contain laminae of sand size calcite. Calcite crystal limestones are common. Near the top of the unit are cut-and-fill structures overlain by current bedded calcite crystal limestones. Also near the top are widespread subvertical clay and calcite crystal veinlets. Calcite nodules are also common throughout Unit 3.

Unit 4 is 2.0m thick and consists largely of claystone and mudstone that are pale yellowish gray to olive gray. There are dispersed sand size calcite crystals and calcite crystal limestones with detrital sand. Two horizons of Magadi-type chert nodules are in the upper part of the unit.

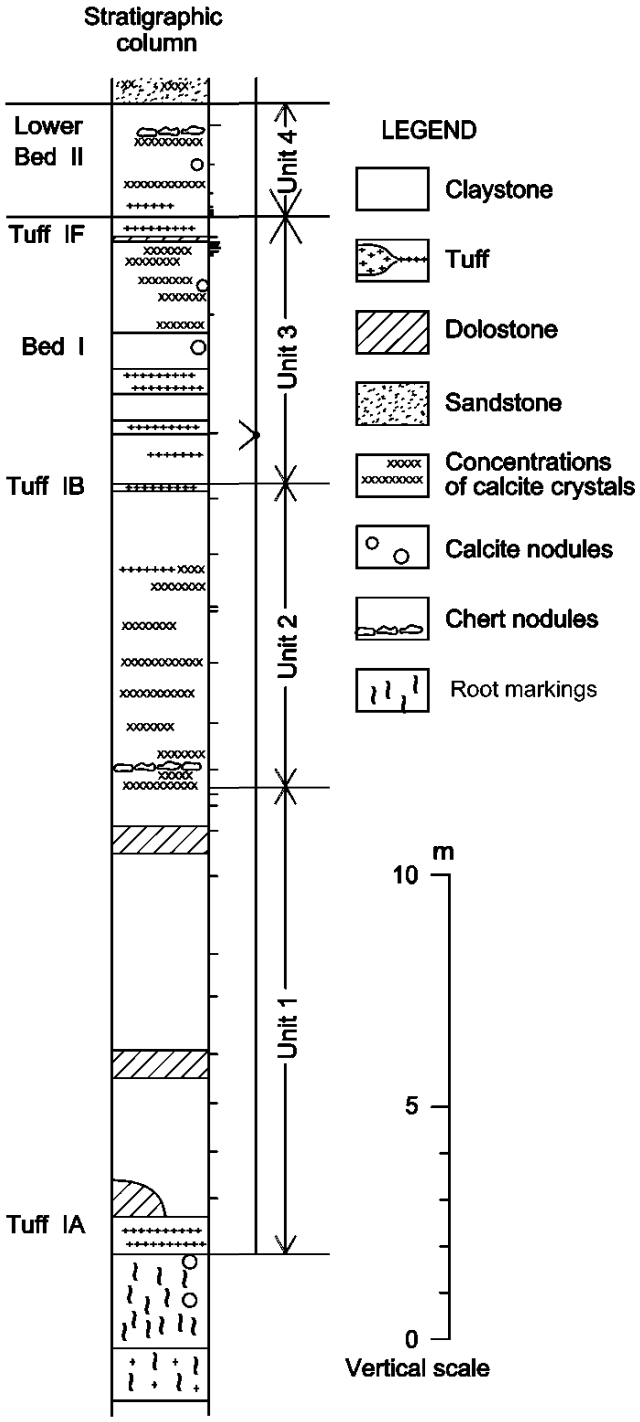

Figure 3 Stratigraphic column at location 80

A columnar section of central basin deposits (modified from (Hay and Kyser, 2001)).

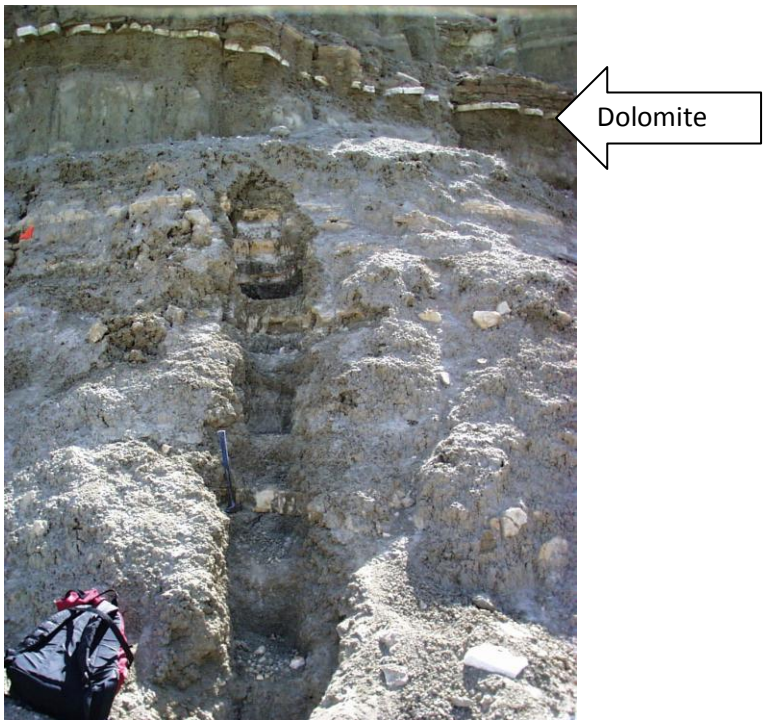

Figure 4 A photograph of Loc 80
The backpack on the fore left of the photograph can be used for scale (source: Ashley, G. (Rutgers University)).

Figure 5 A close up photograph of Loc 80
The hammer in the photograph is included for scale (source: Ashley, G. (Rutgers University)).

Figure 6 A photograph of a section of Location 80 Outcrop
(source: Ashley, G. (Rutgers University)).

1.4 Closed-Basin Lake Hydrology and Geochemical Proxies as Climate Indicators

The geochemical compositions of saline lake waters and sediments are the products of: climate, weathering, groundwater, precipitation dissolution reactions and biotic activity (Yuretich and Cerling, 1983; Yuretich et al., 1986; Rosen, 1994; Yuretich et al., 1995; Calvo et al., 1999; Jones and Deocampo, 2003). A saline lake forms when outflow is absent or restricted; evaporation is greater than or similar to inflow; and inflow is sufficient to maintain a permanent body of water at or near to the surface (Rosen, 1994; Jones and Deocampo, 2003). Saline lakes occur in multiple geographic settings. These areas include the sides of continental uplifts, within extensional and intermontane basins, glaciated terrain and where rain shadows of mountain ranges or highlands provide precipitation catchment and the adjoining basin floor is exposed to evaporation (Jones and Deocampo, 2003).

According to Jones and Deocampo (2003) climate plays a critical role in the water balance of all lakes through inflow, evaporation rates and ambient temperature. Local biota, mineral thermodynamics and open water evaporation are all temperature dependent. The hydrochemistry of a permanent saline body of water will be strongly affected by both typical seasonal variation and monsoonal systems that result in significant lake level fluctuations. Dissolved solids accumulate in the water column as the balance between inflow and evaporation is maintained.

Fundamental controls on the initial chemistry of inflow into closed basins are derived from the lithology of rocks and sediments available for weathering, and groundwater residence times (Yuretich et al., 1986; Rosen, 1994; Cohen, 2003; Jones and Deocampo, 2003). Closed basin brine types throughout the world are controlled by the tectonics on the geology of a watershed (Jones and Deocampo, 2003). Calc-alkaline volcanic activity has dominated East African geology since the Miocene and has produced widespread sodium carbonate waters such as those that were present at the Olduvai Gorge in Plio-Pleistocene time (Renaut et al., 1986; Hover and Ashley, 2003; Jones and Deocampo, 2003; McHenry, 2009).

Solute evolution in saline lake water can be associated with a few fundamental rock types, their reaction with dilute natural waters and the resulting relation of major cations and anions (Jones and Deocampo, 2003). The composition of saline lakes is dominated by Na^{+}, K^{+}, Ca^{2+}, Mg^{2+}, Cl^{-}, SO_4^{2-}, dissolved inorganic carbon as $HCO_3^{-} + CO_3^{2-}$, and rarely SiO_2 (Jones, 1986; Cohen, 2003; Jones and Deocampo, 2003). Evaporation increases the abundance of cations in solution and leads to highly alkaline, high pH waters. The chemical evolution of the saline lake water is then a function of evaporative concentration, mineral precipitation and a number of other processes that can fractionate solutes in these systems (Jones and Deocampo, 2003). These processes include wetting and drying, sulfate reduction, oxidation-reduction of minor minerals, and hydrogen and oxygen isotope dissolution-precipitation fractionation (Cohen, 2003; Jones and Deocampo, 2003).

It must be noted that post depositional change can enhance or obscure the original environmental information (Yuretich and Cerling, 1983; Yuretich et al., 1995; Yuretich et al., 2002). Limitations occur as the saline alkaline water promotes diagenetic reactions in both the detrital and authigenic sediments (Yuretich and Cerling, 1983; Yuretich et al., 1995; Yuretich et al., 2002). Additionally the tectonic activity of the rift valley which causes shifting from one source rock area to another may complicate the paleoclimate archive (Yuretich and Cerling, 1983; Yuretich et al., 2002).

Substantial research has been conducted on the saline alkaline lakes of Africa and the western United States of America. Research areas relevant to this study include Owens Lake, Lake Malawi, Lake Turkana, Lake Albert, Lake Manyara and Paleolake Olduvai. These studies have demonstrated the use of multiple climate proxies and analytical methods for the analysis of lake sediments.

Analytical methods that have been applied in paleolimnological studies include magnetic susceptibility, chemical composition of the carbonate-free clay-sized fraction, X-ray diffraction, stable isotope, geochemical, faunal evidence, the octahedral cation index of authigenic clays, biogenic silica and total inorganic phosphorus (Cerling et al., 1978; Bischoff et al., 1997; Benson et al., 1998; Johnson et al., 2002; Deocampo, 2004; Liutkus et al., 2005; Brown et al., 2007).

1.4.1 Sedimentary Geochemistry: Al_2O_3/MgO ratios

Olduvai Beds I and II at Loc 80 are comprised of 80 percent and 70 percent claystone respectively (Hay, 1976b; Hay, 1981; Ashley and Hay, 2002). The minerals present in the claystone are smectite, Mg-rich authigenic illite and interlayered illite-smectite (Hay and Kyser, 2001). Al-rich smectites are formed by the weathering of basic rocks and are favored by mildly alkaline, lower salinity conditions (Hay et al., 1986; Deer et al., 1992; Webster, 1994; Hay and Kyser, 2001; U.S. Department of the Interior, 2001a; Yuretich et al., 2002). The Al-rich clays found at Loc 80 are more likely of detrital origin whereas the Mg- rich clays are most likely authigenic (Hay and Kyser, 2001).

Illite is formed through wetting and drying of smectite, the weathering of silicates, the alteration of other clay minerals and the degradation of muscovite(Deer et al., 1992; Eberl, 1993; Calvo et al., 1999; Hover et al., 1999; U.S. Department of the Interior, 2001b). Conditions favorable for the formation of illite within lakes are high saline, alkaline waters with high concentrations of Al and K (Hay et al., 1986; Deer et al., 1992; Hay and Kyser, 2001; U.S. Department of the Interior, 2001b). K and Al become concentrated by progressive evaporation whereas Mg^{+2} precipitates into Mg-rich smectite or illite, thus decreasing in solution with increasing pH and alkalinity (Cerling, 1979; Hay et al., 1986; Webster, 1994; Calvo et al., 1999; Hay and Kyser, 2001) Therefore Mg-rich authigenic illite has been used as an indicator of high salinity and high pH lake conditions caused by arid climate (Singer and Stoffers, 1980; Webster, 1994; Hover et al., 2005).

Interlayered illite-smectite (I/S) is a result of smectite illitization, a common mineralogical reaction that occurs during low temperature digenesis, regional metamorphism, wetting and drying of smectite, and hydrothermal alteration (Jones, 1986; Eberl, 1993; Crawford and Haynes, 2002; Hover and Ashley, 2003; Hover et al., 2005; Lanson et al., 2009). At Paleolake Olduvai illitization is most likely due to wetting and drying or early digenesis in saline alkaline fluids. Illitization reaction mechanisms are categorized as either solid-state or dissolution-precipitation transformations (Bethke and Altaner, 1986).The accepted mineralogical sequence has been smectite → randomly interstratified Illite - smectite with high smectite contents (>50% expandable layers) → ordered Illite-expandable with high illite content (>50% Illite layers) → illite (Bethke and Altaner, 1986; Eberl, 1993; Lanson et al., 2009). However, Lanson et al (2009) found that the early stages of smectite illitization are characterized by the coexistence of discrete smectite and of a randomly interstratified illite-expandable with a high content of illite layers. This implies that illitization is a heterogeneous reaction in which a series of intermediate phases occur (Lanson et al., 2009).

Eberl et al (1993) determined that in the absence of temperature, pore-water chemistry exerted a significant control on the smectite to illite reaction. In the presence of K^+ ions and K-minerals, wetting and drying cycles formed, up to 50% expandable randomly interstratified I/S (Eberl, 1993). I/S that formed through a wetting and drying process did not undergo a chemical reaction but rather the illite layers formed in the smectite by mechanical rearrangement and irreversible dehydration of high charge smectite layers around interlayer K^+ (Eberl, 1993). Additionally, the exchange of cations for the calcium lost by carbonate precipitation and reduction of iron increases phyllosilicate layer charge and fixes interlayer cations with potassium and also magnesium (Jones, 1986; Deocampo et al., 2009)

Octahedral positions are also likely places for the accommodation of Mg (Singer and Stoffers, 1980; Deocampo, 2004). Solute loss of potassium and magnesium contributes to the formation of authigenic clays through the transformation of pre-existing clays or through direct mineral precipitation (Jones, 1986; Webster, 1994; Calvo et al., 1999). Magnesium uptake into authigenic clays is enhanced by; reaction with silica from lake waters; lower sedimentation rates; higher salinity and higher pH (Jones, 1986; Webster, 1994; Calvo et al., 1999). Diagenetic alteration of a pre-existing material is a function of the relative insolubilities of the hydroxides of major elements that comprise clay minerals (Jones, 1986). Low Al_2O_3/MgO ratios are used in this study to indicate dry evaporative lake conditions whereas high ratios represent wet lake expansion conditions.

1.4.2 Sedimentary Geochemistry: P_2O_5

According to Cohen (2003) phosphorus is geologically derived from the weathering of phosphate-bearing igneous or sedimentary rocks. Most dissolved phosphorus in lakes occurs as PO_4^{3-}. The compounds are produced through cell excretions, decay of organic matter and release from sediment as soluble reactive phosphorus. Lake bottom sediments can act as both sources and sinks of phosphorus relative to the overlying lake waters. Redox and pH conditions as well as sedimentary Fe

concentrations are the primary controls of phosphorus in the sedimentary record. A higher pH leads to a release of phosphate and possibly reprecipitation as P-minerals or adsorption onto $CaCO_3$.

1.4.3 Sedimentary Geochemistry: TiO_2

TiO_2 represents detrital input from terrigenous source rock (Cohen, 2003). The Titanium supply often increases during periods of rapid erosion and terrestrial sediment discharge (Cohen, 2003). The Ti is released from bedrock under heavy erosional regimes that occur during wet climate conditions (Cohen, 2003). Brown (2011) found that Ti enrichment coincided with the timing of enhanced input of weathered volcanic ash.

1.5 Objective

Testing for the presence of cycles in the bulk geochemical record of Paleolake Olduvai at Locality 80 (loc 80) Central Basin (CB), Tanzania will contribute to the identification of intervals of wet/dry climatic conditions. The majority of the sediments at Loc 80 are illite, smectite, and I/S, therefore an emphasis is placed on the analysis of the relationships between the following oxides and their ratios, Al_2O_3/MgO, TiO_2 and P_2O_5. X-ray Fluorescence (XRF) spectroscopy was used to collect the geochemical data from the sediments. The data are compared to previously published articles for consistency. The study will contribute to the continued efforts to reconstruct paleoclimate and the exploration into the cause(s) of the climatic variations which controlled inflow and evaporation.

2. METHODS

2.1 Samples

The stratigraphic section at Loc 80 and 167 sediment samples were provided by Dr. Gail Ashley of Rutgers, The State University of New Jersey. The Stratigraphic section was logged and the sediment samples were collected from a freshly excavated outcrop and stored in plastic bags, on, July 9-11, 1999 by G.M. Ashley, R.W. Renaut and R.L. Hay in collaboration with the Olduvai Landscape Paleoanthropology Project (OLAPP).

2.2 Age Model

The age model is based on the published dates by Hay and Kyser (2001) for Tuff IA, Tuff IB, Tuff IF, the chert nodules and the disconformity. Additionally the Hay and Kyser (2001) sedimentation rates for age determination, 1 m = 5900 yr for units 1 and 2 and 1 m = 8300 yr for units 3 and 4, were used to determine the number of years required for each cycle to complete. These sedimentation rates are based on the paleomagnetic stratigraphy which contains the Olduvai (normal) Subchron. The lower limit of the subchron occurs six meters below Tuff IA. There are four meters of tuff and two meters of claystone between the base of the subchron and Tuff IA (Hay and Kyser, 2001). Hay and Kyser (2001) use an arbitrary sedimentation rate of 30cm/k.y. to determine an age of 1.92 Ma for Tuff IA. After revising the tuff dates to fit the Olduvai Subchron, Hay and Kyser (2001) determine the sedimentation rate of nontuff lithologies from Tuff IA to Tuff IB to be 17 cm/k.y. for the CB in present day compacted thickness. For the nontuff lithologies between Tuff IB and Tuff IF the sedimentation rate is 12 cm/k.y..

2.3 Geochemistry X-ray Fluorescence (XRF)

X-ray fluorescence (XRF) analyses were conducted on 167 sediment samples from Loc 80. The following process was performed on each individual sample. Using a mortar and pestle the whole rock sample was powdered. Then 0.500 grams of powdered rock sample was combined with 4.500 grams of lithium tetraborate ($Li_2B_4O_7$). The combined sample was fused into a glass disk at 1100° C. Major and

trace element analyses were conducted at Georgia State University with a Rigaku 3270 wavelength dispersive X-ray spectrometer operated at 50mA and 50kV (Appendix A).

Analytical error was estimated using United States Geological Survey (USGS) standard reference material BHVO1 (basalt). The standard was analyzed at the beginning of each day of use of the Rigaku 3270 wavelength dispersive spectrometer and error estimates were made for each major element oxide and trace elements (Appendix C).

Instrumental drift was identified through analysis of the USGS BHVO1 standard. The effect was most significant with regard to the SiO_2 weight percentages. Future studies that reference this data should correct for the instrumental drift by using the standard analysis for each batch. The data was normalized (Appendix B) using the following formula, 100*(weight percent of selected oxide for the selected sample)/ (sum of all weight percents of the oxides for the selected sample) =normalized oxide weight percent. Example: 100*(SiO_2 weight percent for sample 171)/ (the sum of the weight percents SiO_2 +TiO_2+Al_2O_3+Fe_2O_3+MnO+MgO+CaO+Na_2O+K_2O+$P2O_5$ from sample 171) =normalized oxide weight percent for SiO_2 for sample 171.

2.4 Loss on Ignition (LOI)

Loss on ignition is a method used to estimate the organic matter, carbonate content and clay content associated with lake sediments (Heiri et al., 2001; Cohen, 2003; Santisteban et al., 2004). LOI_{550} can represent both the percent of organic matter present in the sediment and the lattice water in clays; whereas LOI_{950} is representative of the percent of carbonate present within the sediment (Heiri et al., 2001; Santisteban et al., 2004). Most carbonate minerals are destroyed at 950^{o}C (Santisteban et al., 2004). At 200^{o}C organic matter begins to ignite and is completely oxidized at approximately 550^{o}C (Heiri et al., 2001). Lattice water or structure water in clays is lost at 550^{o}C (Santisteban et al., 2004). The primary clay minerals at Loc 80 are illite and smectite both of which are hydrous and thus will lose

structural water on ignition. It is reasonable therefore to expect a strong correlation between LOI_{550} and Al_2O_3 or MgO depending on the oxide present in the clay.

Loss on Ignition (LOI) was conducted at 550 °C and 950 °C on 56 of the 167 sediment samples. Each sample was weighed and then heated to 550 °C for two hours and reweighed. The samples were then heated for an additional two hours at 950 °C and weighed.

When removed from the oven after heating at 550^{oC}, the samples were not placed in a desiccator to cool and no measures were taken to ensure that the samples did not absorb water from the air. The weight of the samples was measured when the samples had cooled enough to handle comfortably with gloves, but were not allowed to cool thoroughly prior to weight measurement. More notably, the samples were not dried overnight to remove water. Although the crucibles were always heated and dried for several minutes after washing them, the samples themselves were moved immediately from storage into the oven for analysis. Finally, the procedure was not exhaustive. The samples were not heated any additional times for more measurements to be certain that all volatile content had been removed. LOI calculations were based on those of Heiri et al (2001), LOI_{550}= ((DW-DW_{550})/DW)*100, where LOI_{550} represents LOI at 550°C as a percentage, DW represents the dry weight of the sample before combustion and DW_{550} is the dry weight of the sample after combustion. LOI_{950}= ((DW_{550}-DW_{950})/DW)*100, where LOI_{950} represents LOI at 950°C as a percentage, DW_{550} represents the dry weight of the sample after combustion at 550°C and DW_{950} is the dry weight of the sample after heating to 950°C and DW represents the dry weight of the sample before combustion. Major element oxide data from XRF analysis was compared to LOI results (Appendix A).

3. RESULTS

3.1 Geochemistry X-ray Fluorescence (XRF)

One hundred sixty seven sediment samples were analyzed using XRF spectroscopy and the results are listed in Appendix A, Appendix B and Appendix D. A significant portion of the data collected

will not directly contribute to this study but will be a collaborative contribution to the Olduvai Landscape Paleoanthropology Project (OLAPP).

Patterns in the weight percentages of Al_2O_3/MgO, TiO_2 and P_2O_5 show that the peak lows and peak highs occur at, or nearly at, the same elevation within the stratigraphic section. Low weight percentages of the oxides indicate saline alkaline conditions whereas high weight percentages represent fresh water conditions. The mean, standard deviation and range of values for each oxide is listed in Table 1.

Table 1 Mean, Standard Deviation and Range of Values for Selected Oxides

Oxide	Al_2O_3	MgO	TiO_2	P_2O_5
Mean	14.92	9.20	2.93	0.38
Standard Deviation	0.23	0.41	0.10	0.01
+/- %	1.55	4.45	3.58	3.29
Range of Values	2.93-17.81	0.96-34.30	0.34-2.09	0.05-0.41

3.1.1 Relationships between Selected Oxides

There are no significant correlations between the oxides (Figure 7, Figure 8, Figure 9).

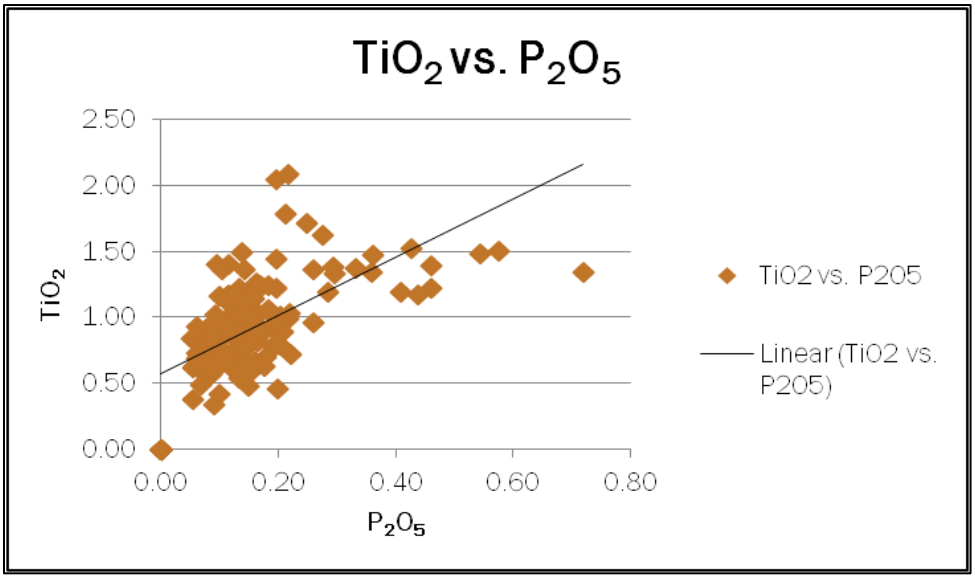

Figure 7 A scatter plot of the relationship between oxides, TiO_2 vs. P_2O_5.
There is no significant correlation between the oxides.

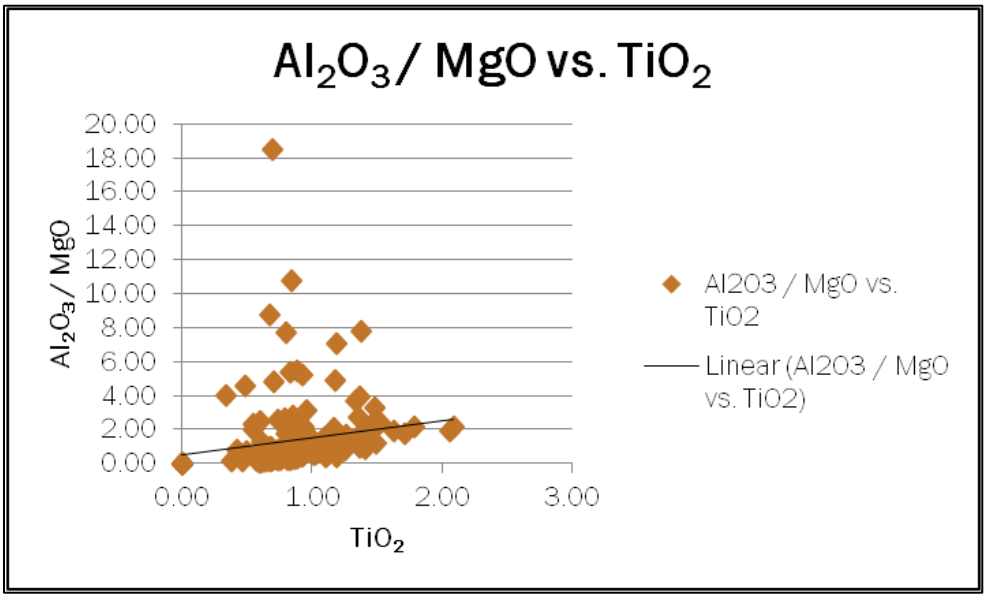

Figure 8 A scatter plot of the relationship between oxides, Al_2O_3/MgO vs. TiO_2.
There is no correlation between the oxides.

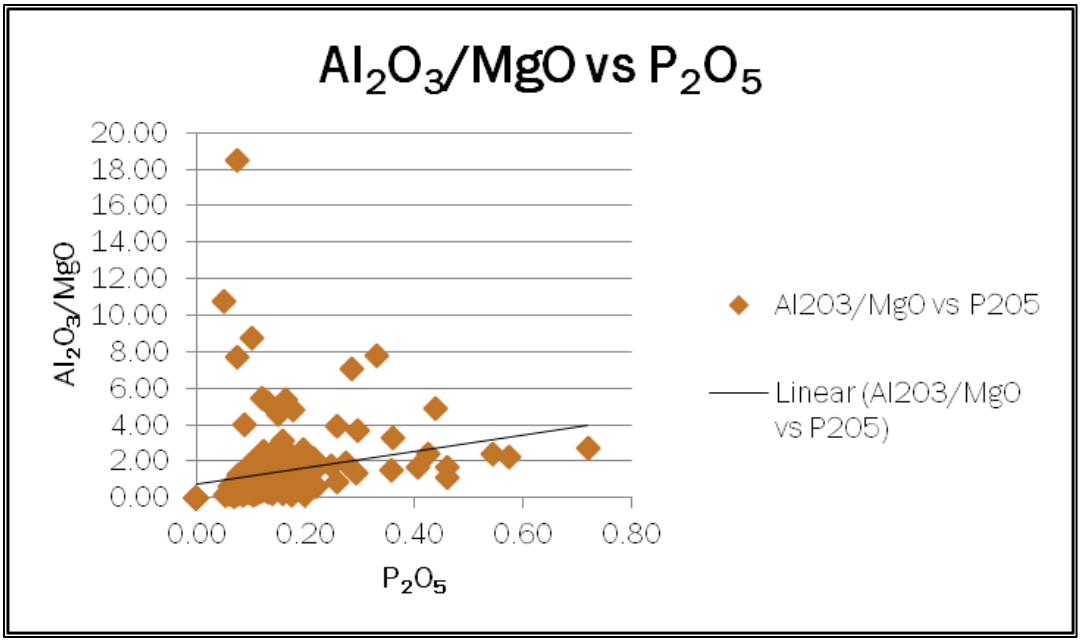

Figure 9 A scatter plot of the relationship between oxides, Al_2O_3/MgO vs. P_2O_5
There is no correlation between the oxides

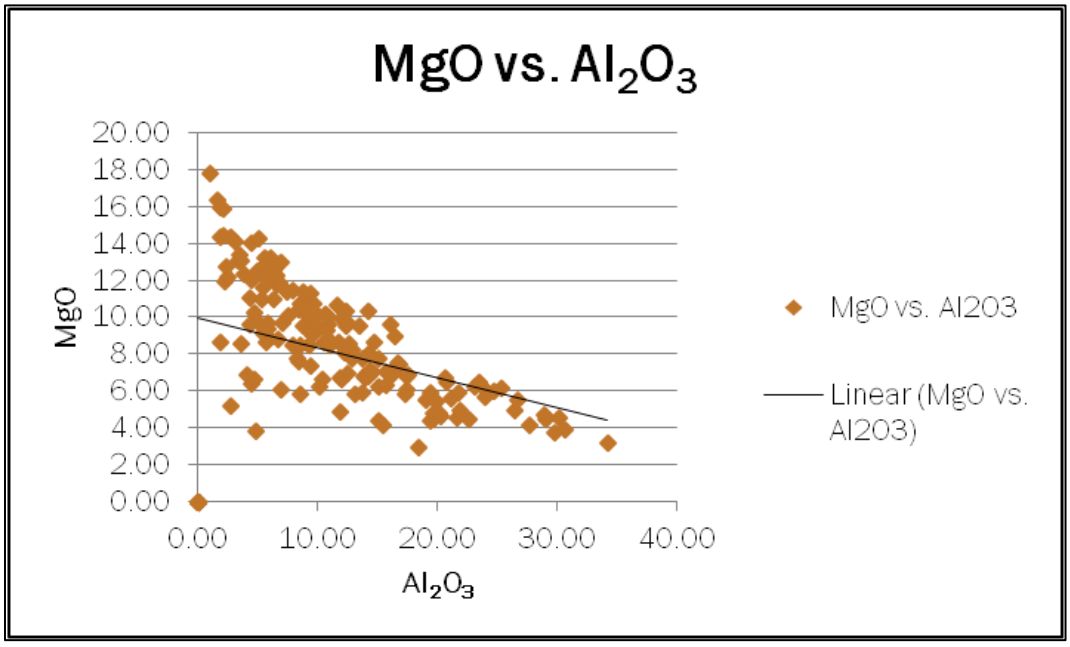

Figure 10 A scatter plot of the relationship between oxides, Al_2O_3 vs. MgO
There is no correlation between the oxides

3.1.2 Abundance of Oxides and Position in the Stratigraphic Column

Al_2O_3/ MgO weight percent ratios, along withTiO_2 and P_2O_5 weight percentages were plotted against meters from the bottom of the section. The plot was divided into Bed I and Lower Bed II, Units 1-4 and the locations of Tuff IA, Tuff IB, Tuff IF, chert nodules and a disconformity. There is an oscillating pattern of increasing and decreasing abundance of oxide weight percent per depth that is similar across all three plots (Figure 11, Figure 12, Figure 13). Below Tuff IA, TiO_2, Al_2O_3/MgO and P_2O_5 decrease, up-section, in the weight percent of the oxides.

Al_2O_3/MgO, TiO_2 and P_2O_5 follow an almost identical pattern with some minor variations in the location of occurrence. Peak lows in the weight percent Al_2O_3/MgO occur at approximately 6m, 12.5m, 17.5m, 21m and 26m and peak highs occur at approximately 3.8m, 11m, 16m, 20m, 24m and 30m (Table 2). The peaks oxide ratios at the lowest points for Al_2O_3/MgO ranged from 0.13 to 0.56 while the highest points ranged from 0.78 to 4.00.

Lows in the weight percent TiO_2 occur at approximately 6m, 14m, 18m, 21m and 28m and peak highs occur at approximately 2m, 11m, 15.9m, 20m, 23m and 30m (Table 3). The weight percent of oxide present at the lowest points for TiO_2 ranged from 0.46 to 0.73 and the highest points range from 1.16 to 1.62.

Peak lows in the weight percent of P_2O_5 occur at approximately 6m, 14m, 17m, 24m and 27.5m and peak highs occur at approximately 3.8m, 11m, 16m, 21m, 26m and 30m. The weight percent of oxide present at the lowest points for P_2O_5 ranged from 0.05 to 0.08 while the highest points ranged from 0.18 to 0.60 (Table 4).

The elevation at occurrence values in tables 2, 3 and 4 were averaged and plotted as Y coordinates and the weight percent values were averaged and represent the X coordinates. The points were connected with a smooth curve representing the lake cycles in Figure 17.

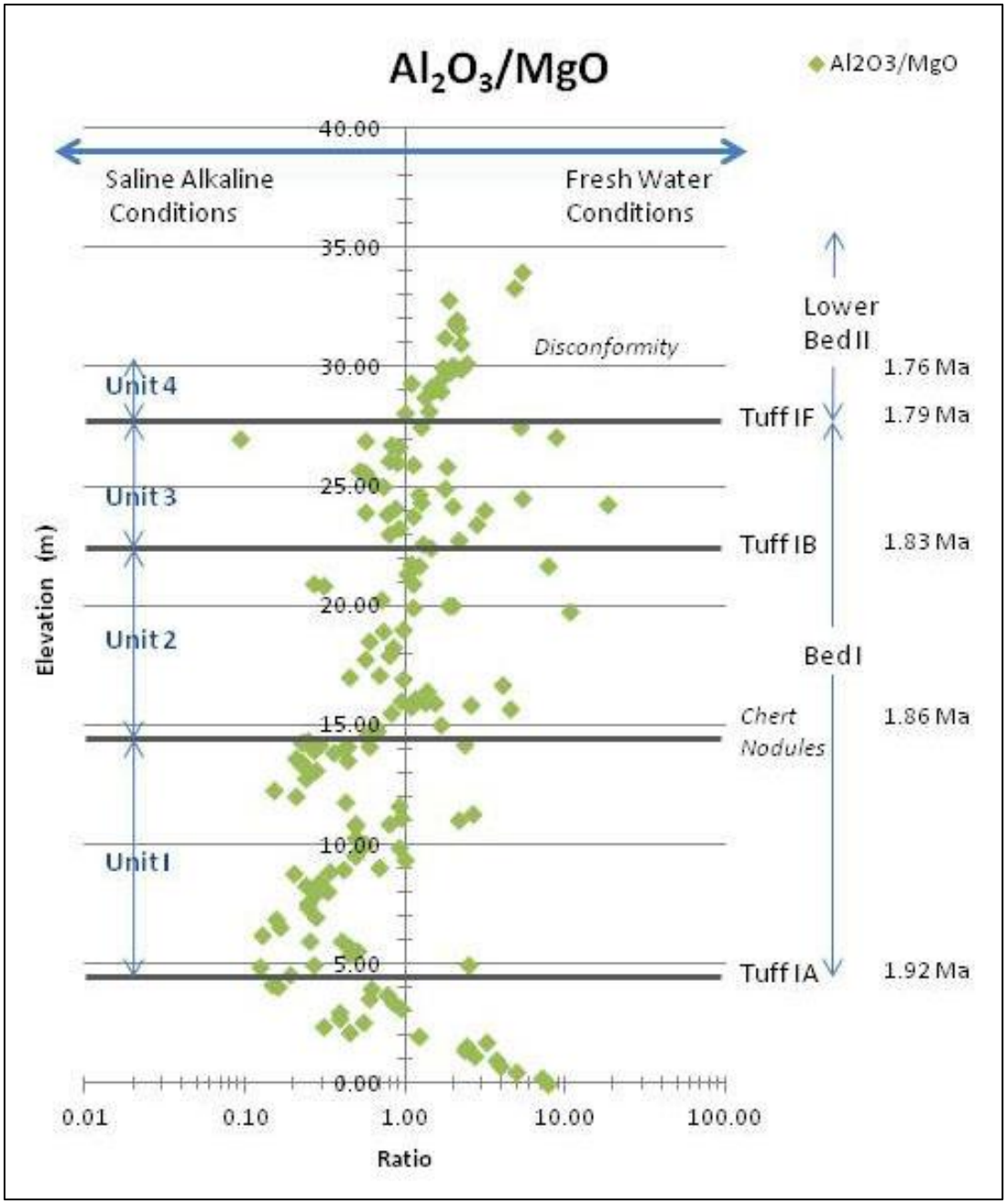

Figure 11 Al_2O_3/MgO and the Stratigraphic Column

The trends in lake water conditions as represented by the sedimentary record are presented with corresponding elevation within the stratigraphic column and location of samples. Major stratigraphic markers- Tuff IA, Tuff IB, Tuff IF, the presence of chert nodules and the lower most disconformity are represented along with Bed I and Bed II, the division of Units 1, 2, 3 and 4 and relative geologic ages.

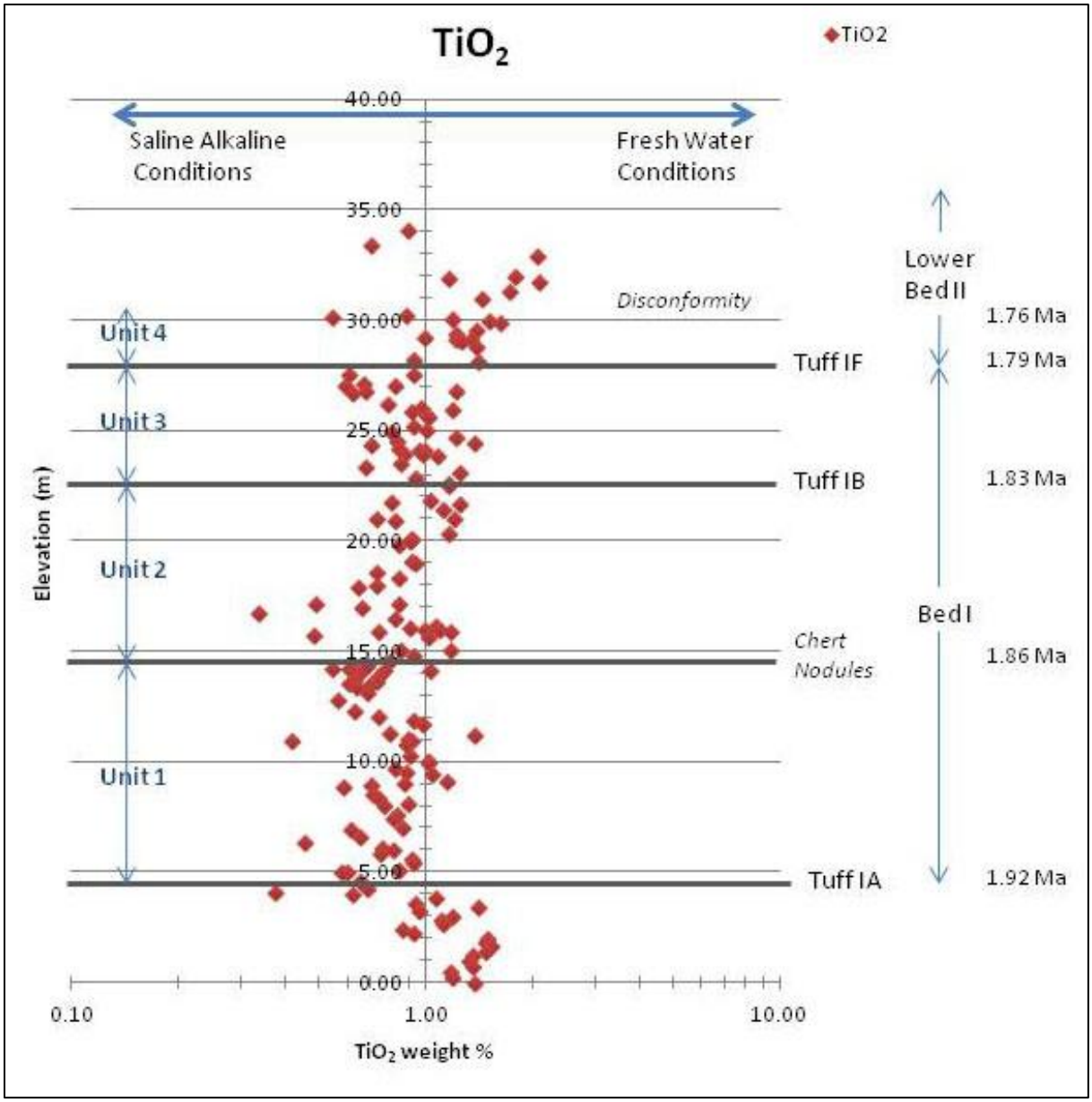

Figure 12 TiO_2 and the Stratigraphic Column

The trends in lake water conditions as represented by the sedimentary record are presented with corresponding elevation within the stratigraphic column and location of samples. Major stratigraphic markers- Tuff IA, Tuff IB, Tuff IF, the presence of chert nodules and the lower most disconformity are represented along with Bed I and Bed II, the division of Units 1, 2, 3 and 4 and relative geologic ages.

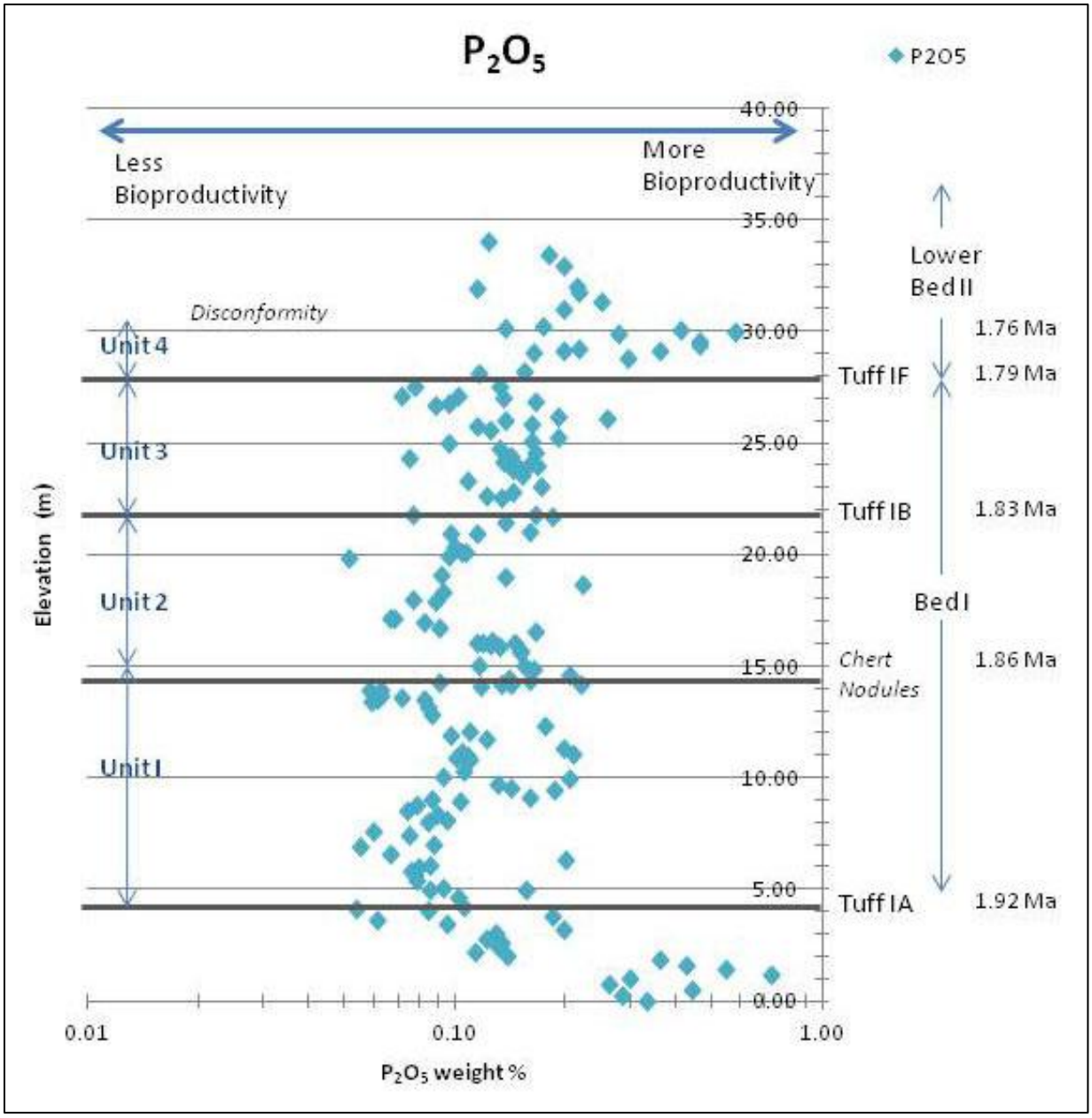

Figure 13 P_2O_5 and the Stratigraphic Column

The trends in lake water conditions as represented by the sedimentary record are presented with corresponding elevation within the stratigraphic column and location of samples. Major stratigraphic markers- Tuff IA, Tuff IB, Tuff IF, the presence of chert nodules and the lower most disconformity are represented along with Bed I and Bed II, the division of Units 1, 2, 3 and 4 and relative geologic ages.

Table 2 Al_2O_3/MgO weight percent peak highs and lows with elevation at occurrence.

Al_2O_3/MgO				
UNIT	Oxide Weight % Peak Low	Elevation at Occurrence	Oxide Weight % Peak High	Elevation at Occurrence
1	0.13	6.0	0.78	3.8
1	0.15	12.5	2.14	11.0
2	0.45	17.5	4.00	16.0
2	0.27	21.0	2.00	20.0
3	0.56	26.0	3.13	24.0
4	undefined	undefined	2.39	30

Table 3 TiO_2 weight percent peak highs and lows with elevation at occurrence.

TiO_2				
UNIT	Oxide Weight % Peak Low	Elevation at Occurrence	Oxide Weight % Peak High	Elevation at Occurrence
1	0.46	6.0	1.49	2.0
1	0.54	14.0	1.37	11.0
2	0.64	18.0	1.17	15.9
2	0.73	21.0	1.16	20.0
3	0.61	28.0	1.25	23.0
4	undefined	undefined	1.62	30.0

Table 4 P_2O_5 weight percent peak highs and lows with elevation at occurrence.

P_2O_5				
UNIT	Oxide Weight % Peak Low	Elevation at Occurrence	Oxide Weight % Peak High	Elevation at Occurrence
1	0.05	6.0	0.18	3.8
1	0.06	14.0	0.20	11.0
2	0.07	17.0	0.60	16.0
2	0.08	24.0	0.18	21.0
3	0.08	27.5	0.26	26.0
4	undefined	undefined	0.41	30.0

3.2 Loss on Ignition (LOI)

Samples heated for 2 hours at 550°C yielded LOI from 0.2-10.2 percent. Samples heated for 2 hours at 950°C lay within an LOI range of 0.3-11.9 percent. CaO (carbonate) from XRF was plotted against LOI_{950} resulting in a positive correlation and a R^2 (correlation coefficient) value of 0.75 (Figure 14). Al_2O_3 (representing clay minerals) was plotted against LOI_{550} resulting in no correlation (Figure 15). MgO (representing clay minerals) was both plotted against LOI_{550} and resulted in a positive correlation with a R^2 value of 0.69 (Figure 16).

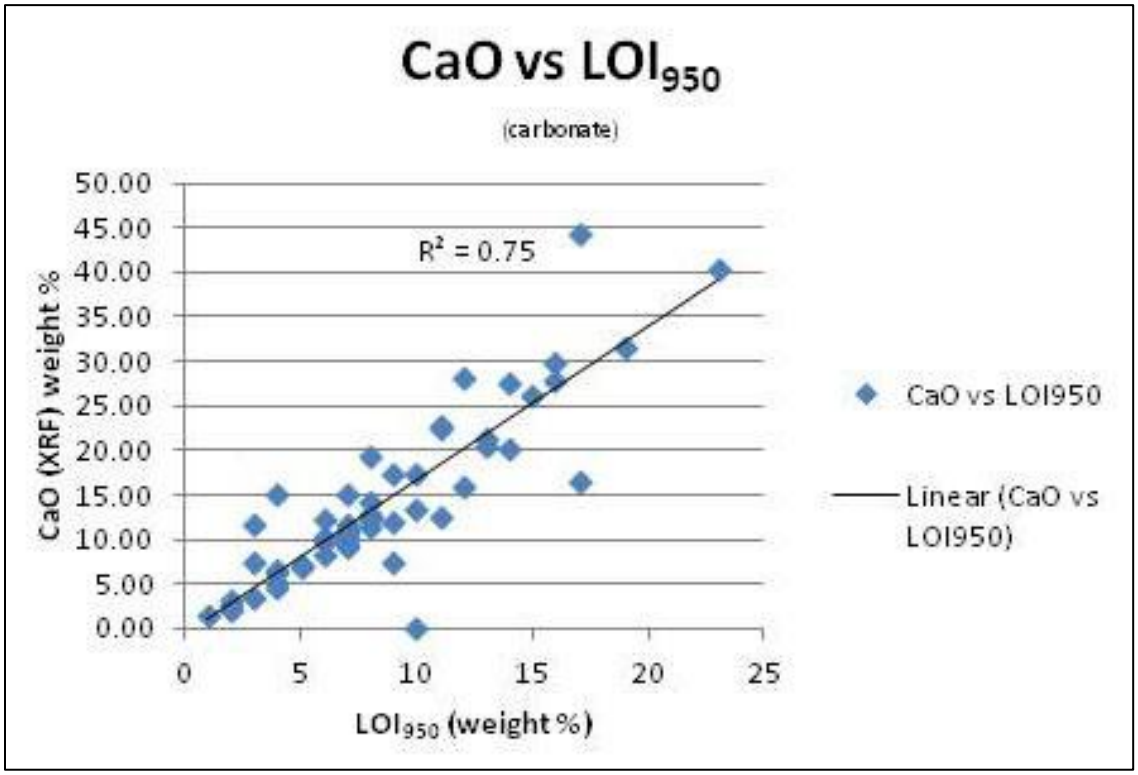

Figure 14 CaO vs. LOI_{950}
A positive relationship with R^2 value of 0.75 indicates the presence of carbonates in the sediments.

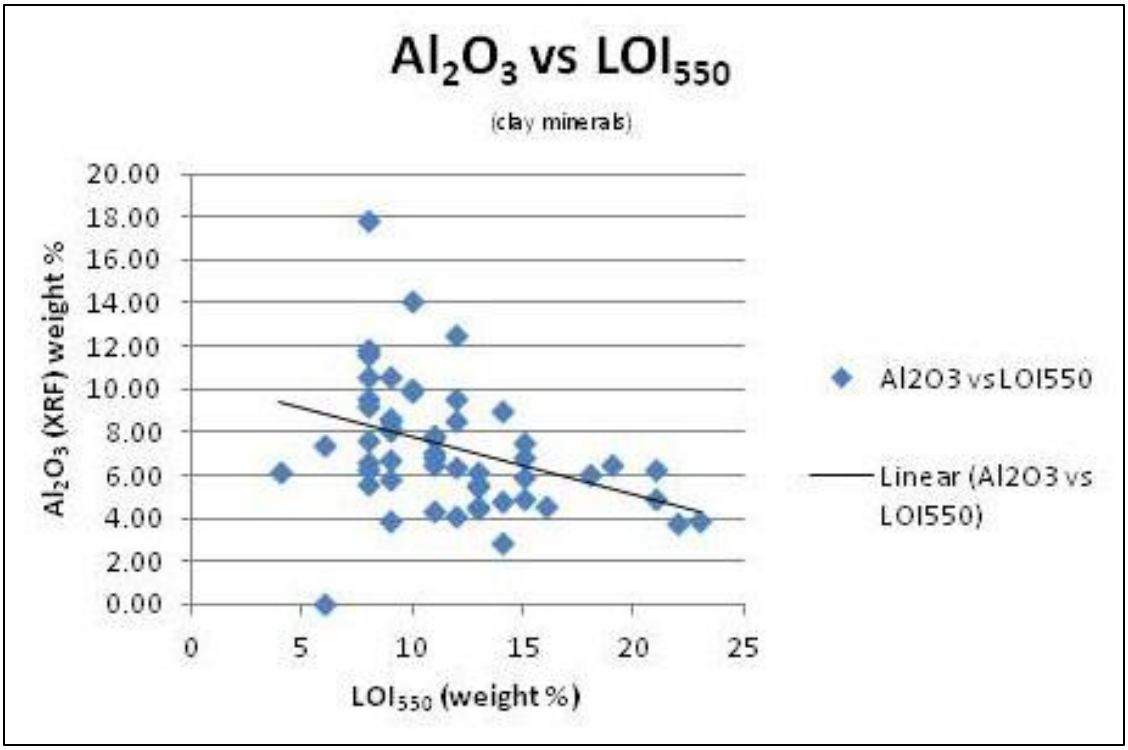

Figure 15 Al_2O_3 vs. LOI_{550}

No correlation implies that bulk Al_2O_3 content is not directly related to clay content.

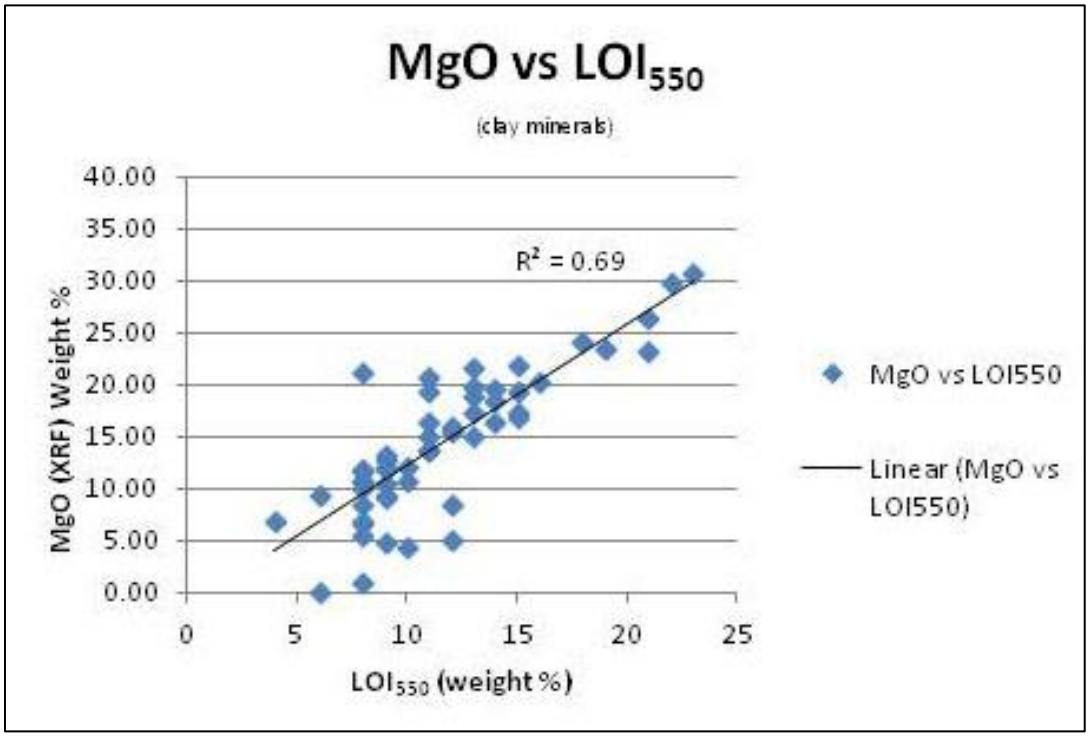

Figure 16 MgO vs. LOI_{550}

A positive relationship with an R^2 value of 0.69; the strong correlation implies the presence of magnesium rich clay due to water loss in the clay lattice. The MgO content increases with the increase in clay present.

4. DISCUSSION

4.1 Clay Minerals and Carbonates

Previous work indicates that the clays of the CB are Mg-rich and that the presence of dolomite is very limited. This study demonstrates a positive MgO vs. LOI_{550} relationship with an R^2 value of 0.69. The strong correlation implies the presence of magnesium rich clay due to water loss in the crystal lattice. The MgO content increases with the increase in presence of clay and is unlikely to be the result of dolomite. Calcite and limestones are found throughout Loc 80 and the LOI average for CO_2 is 3.65 percent. Al_2O_3 vs. LOI_{550} shows no correlation and the bulk Al_2O_3 content is not directly related to clay content.

Phosphorus highs correlate with the fresh water phases as determined by the TiO_2 and the Al_2O_3/MgO ratios. The high pH conditions are considered the driving force that aided the release of phosphorus from the sediment and thus availability to salt tolerant organisms. The lower saline / pH conditions allowed for an increase in biological activity. The phosphorus peaks may be slightly different from the peaks of Al_2O_3/MgO and TiO_2 due to a delay in response by biologic activity. Brown (2011) also found a lag in the onset of wetter conditions and the increase in diatom productivity.

4.2 Lake Cycles

Major oxide analysis shows four major lake cycles (Figure 17 and Figure 19). Each lake cycle begins and ends with a saline alkaline or dry phase. The Hay and Kyser (2001) sedimentation rates for age determination, 1 m = 5900 yr for units 1 and 2 and 1 m = 8300 yr for units 3 and 4, were used to determine the number of years required for each cycle to complete (Table 5, Figure 17). Lake Cycle (LC) 1 completed in approximately 44,000 yrs, LC 2 completed in approximately 24,000 years, LC 3 completed in approximately 24,000 years and LC 4 completed in approximately 42,000 years.

The lake cycles presented here are of higher resolution than those of Hay and Kyser (2001) (Figure 18). However the general trends of fresh water conditions / higher average lake level and saline

alkaline conditions / lower lake level are complimentary (Figure 18 and Figure 19). Unit 1 in this study has 0.5 lake cycles, whereas Unit 1 in Hay and Kyser 2001 shows only an elevated lake level; the trend however in this study remains that of freshening water conditions throughout unit 1 and thus would agree with lake level remaining high. Unit 2 reflects two lake cycles that correspond evenly with both this study and that of Hay and Kyser (2001). The data for Unit 3 in this study are more difficult to interpret and have greater scatter. It appears as though there is one lake cycle that occurs within Unit 3 with a general trend toward saline alkaline conditions. Hay and Kyser (2001) demonstrate a consistently low lake level with two significant lake level drops. There are two points of high lake level in Unit 4 for Hay and Kyser (2001). However, Unit 4 for this study contains only one half of a lake cycle and trends toward saline alkaline conditions only. The general trend for Loc 80 determined by previous research is one of aridity and this study supports this trend.

The variations that occur with regard to peak highs and peak lows at elevation of occurrence can be explained by the amount of time it takes for each constituent in the system to respond to the changing chemistry of the lake water due to climate fluctuations. During wet seasons TiO_2 responds slightly before Al_2O_3/MgO and P_2O_5 and during dry seasons Al_2O_3/MgO responds slightly before TiO_2 and P_2O_5.

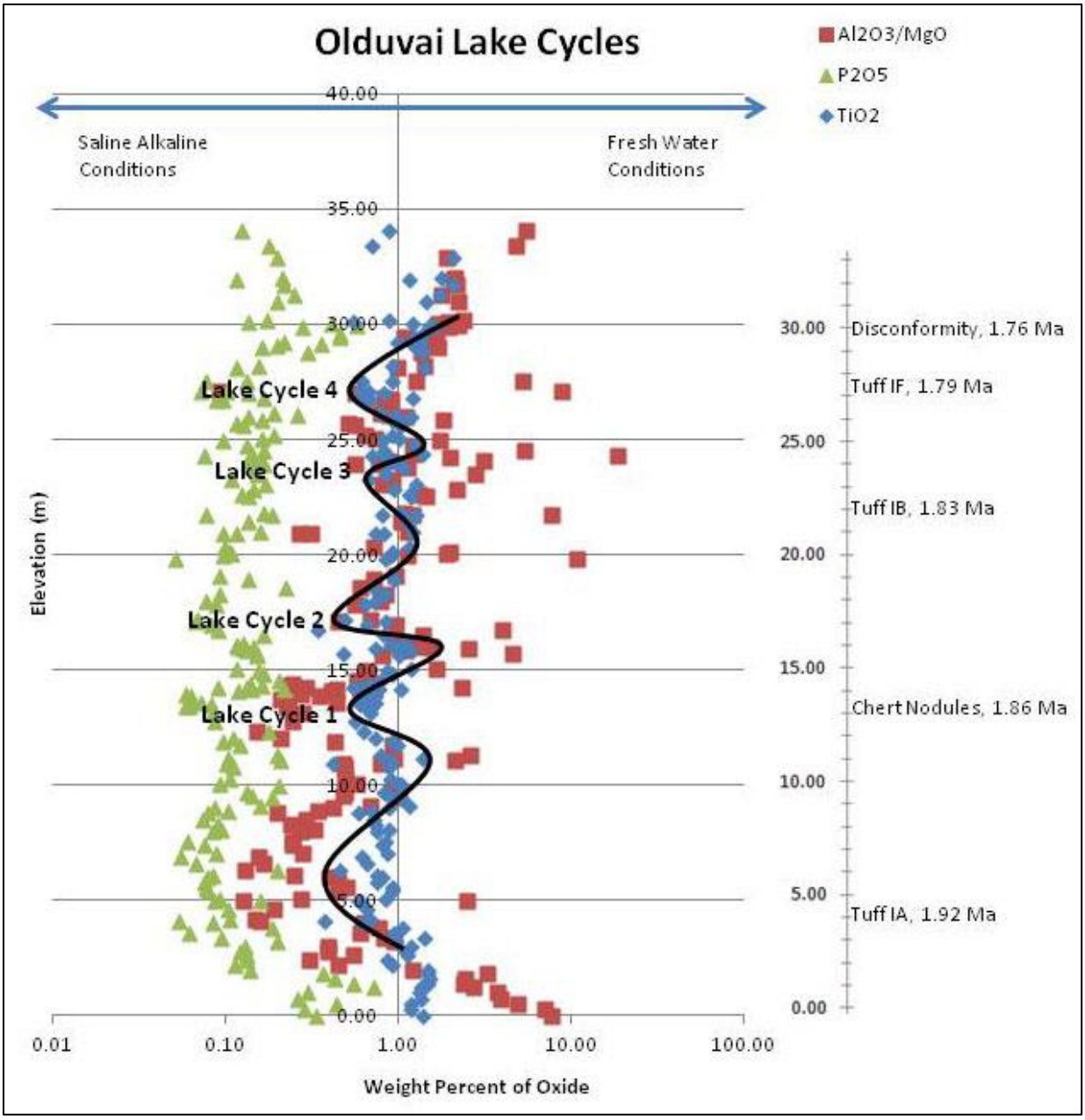

Figure 17 Paleolake Olduvai Cycles: Five complete lake cycles are represented.

Major oxide analysis demonstrates four major lake cycles. Each lake cycle begins and ends with a saline alkaline or dry phase. The Hay and Kyser (2001)sedimentation rates for age determination, 1 m = 5900 yr for units 1 and 2 and 1 m = 8300 yr for units 3 and 4, were used to determine the number of years required for each cycle to complete. Lake Cycle (LC) 1 completed in approximately 44,250 yrs, LC 2 completed in approximately 23,600 years, LC 3 completed in approximately 26,550 years and LC 4 completed in approximately 41,500 years. The average Lake Cycle is 33,975 years.

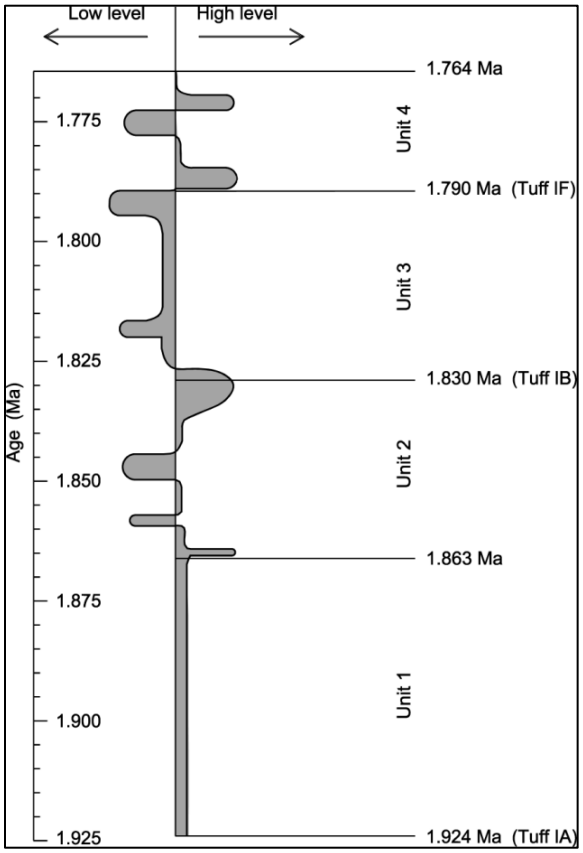

Figure 18 Inferred episodes of higher and lower average lake levels for Paleolake Olduvai.
Central basin at locality 80, after (Hay and Kyser, 2001)

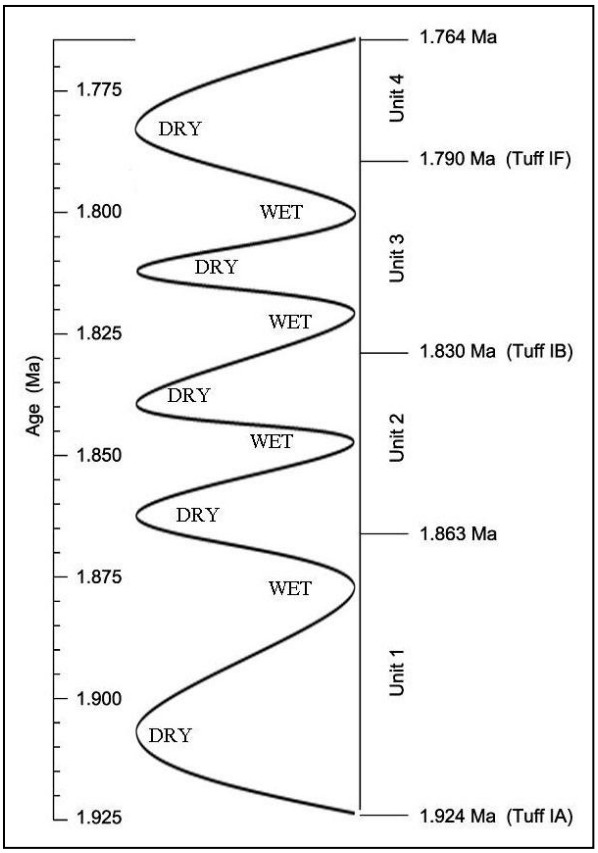

Figure 19 Wet / Dry Lake Cycles
Central basin at locality 80- inferred episodes of wet/dry cycles based on major oxide analysis.

Table 5 Approximate time in years that it takes for each lake cycle to complete.

UNIT	Lake Cycle	Meters	Approx. Years by Sed Rate
1	1	7.5	44,000
1 & 2	2	4	24,000
2	3	4.5	24,000
3	4	5	42,000
Sed Rate (Hay and Kyser 2001): Units 1 & 2, 1m=5900yrs ; Units 3 & 4, 1m=8300yrs			

4.3 Paleoenvironmental Implications

Multiple studies have found that East African hominin evolution coincides with large scale shifts in climate (Trauth et al., 2005; Trauth et al., 2007). Evolutionary developments between 1.9 Ma and 1.7 Ma include the first appearance of *Homo erectus* and *Homo ergaster* as well as the extinction of *Homo habilis* and *Homo rudolfensis* (Figure 20) (Trauth et al., 2005; Trauth et al., 2007). The first hominin exodus out of Africa and into Europe and South Asia also occurred at this time (DeMenocal, 2011).

Climate change produce shifts in the ecological structure of an environment which affects both vegetation and resource availability (Trauth et al., 2007; DeMenocal, 2011). These environmental modifications provide the stress required to initiate speciation (Trauth et al., 2005). The significant fluctuations of Paleolake Olduvai identified in this study are reflections of a dramatically changing climate and environment. In order to survive the Olduvai hominins would have had to adapt or risk certain demise. Ashley et al (2009) demonstrated the use of springs and wetlands by hominins during dry conditions. As food and potable water availability changed the hominins were forced to adjust their subsistence patterns (Ashley et al., 2009). Without question environmental shifts had significant impact on the flora and fauna of Paleolake Olduvai.

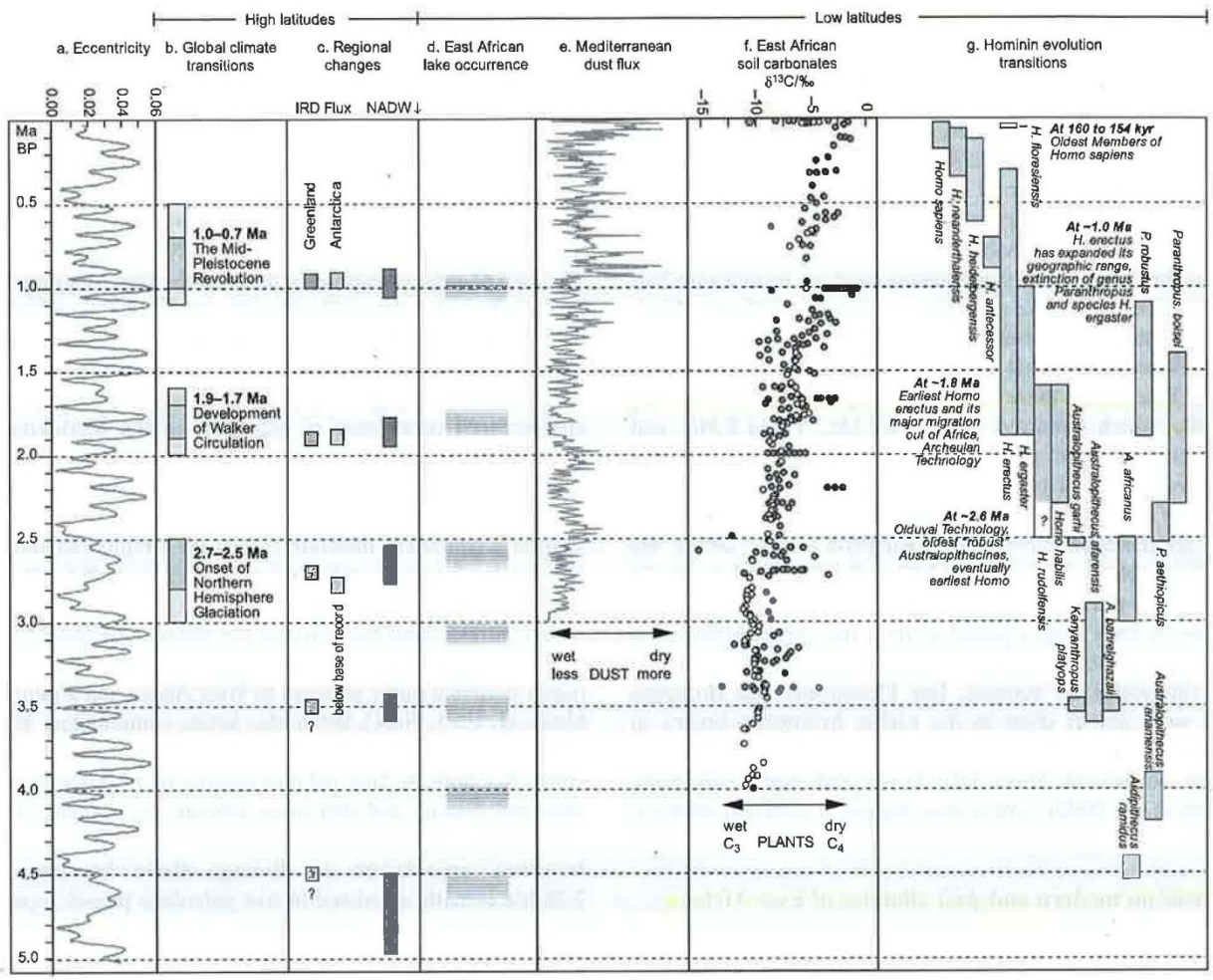

Figure 20 Environmental Factors and Hominin Evolution

Comparison of eccentricity, climate transitions, Mediterranean dust flux, soil carbonate isotopes, East African lakes and hominin evolution after (after (Trauth et al., 2007)

4.4 Future Work

Research at the Olduvai Gorge is ongoing. Using the data set obtained through this study there are numerous opportunities to examine relationships between the oxides, as well as compare the data to the insolation record and to other paleoclimate records. Additional data collection, from the Loc 80 samples, through loss on ignition and X-Ray Diffraction (XRD) would provide a more complete look at the lake cycles. Possible causes of the climatic variations such as tectonics and orbital forcing should be explored.

5. CONCLUSIONS

Strong geochemical correlations were found between the oxides and four apparent lake cycles were identified for Paleolake Olduvai between 1.92 Ma and 1.76 Ma. Similar to the findings of Deocampo (2004) there are correlations with obliquity and precession. However some environmental oscillations occur independently of those controls and may be the result of local variations in insolation (Trauth et al., 2005). The Lake Cycles 1 (44,000 yrs) and 4 (42,000 yrs) are similar to the 41k.y. year cycle associated with Earth's obliquity, which has a direct impact on climate cycles (deMenocal, 1995; Deocampo, 2004). However the impact of obliquity on low latitude locations such as the Olduvai Gorge is not usually considered as significant as precession (deMenocal, 1995; Deocampo, 2004; Ashley, 2007; Ashley et al., 2009). Lake Cycle 2 (24,000yrs) and LC 3 (24,000yrs) are similar to the 21k.y. precession cycle. The general climate trend is toward that of aridity. Both remote and local acting mechanisms impact the climate cycles at Paleolake Olduvai. Further analysis is imperative to provide a complete history of this complex system.

6. REFERENCES

Ashley, G. M., 2007, Orbital rhythms, monsoons, and playa lake response, Olduvai Basin, equatorial East Africa (ca. 1.85-1.74 Ma): Geology, v. 35, no. 12, p. 1091-1094.

Ashley, G. M., and Hay, R. L., 2002, Sedimentation Patterns in a Plio-Pleistocene Volcaniclastic Rift Platform Basin, Oluvai Gorge, Tanzania: SEPM Special Publication No. 73, p. 107-122.

Ashley, G. M., Tactikos, J. C., and Owen, R. B., 2009, Hominin use of springs and wetlands; paleoclimate and archaeological records from Olduvai Gorge (approximately 1.79-1.74 Ma): Palaeogeography, Palaeoclimatology, Palaeoecology, v. 272, no. 1-2, p. 1-16.

Benson, L. V., May, H. M., Antweiler, R. C., and Brinton, T. I., 1998, Continuous Lake-Sediment Records of Glaciation in the Sierra Nevada between 52,600 and 12,500 ^{14}C yr B.P.: Quaternary Research, v. 50, p. 113-127.

Bethke, C. M., and Altaner, S. P., 1986, Layer-by-Layer Mechanism of Smectite Illitization and Application to a New Rate Law: Clay and Clay Minerals, v. 34, no. 2, p. 136-145.

Bischoff, J. L., Fitts, J. P., and Fitzpatrick, J. A., 1997, Responses of sediment geochemistry to climate change in Owens Lake sediment: An 800-k.y. record of saline/fresh cycles in core OL-92: Geological Society of America Special Papers, v. 317, p. 37-47.

Brown, E. T., Johnson, T. C., Scholz, C. A., Cohen, A. S., and King, J. W., 2007, Abrupt change in tropical African climate linked to the bipolar seesaw over the past 55,000 years: Geophysical Research Letters, v. 34, no. L20702.

Calvo, J. P., Blanc-Valleron, M. M., Rodriguez-Arandia, J. P., Rouchy, J. M., and Sanz, M. E., 1999, Authigenic Clay Minerals in Continental Evapoitic Environments: in Thiry, M., and Simon-Coincon, R., eds., Palaeoweathering, palaeosurfaces, and related continental deposits: Special Publication, International Association of Sedimentologists, Wiley, p. 129-151.

Cerling, T. E., 1979, Paleochemistry of Plio-Pleistocene Lake Turkana, Kenya: Paleogeography, Paleoclimatology, Paleoecology, v. 27, p. 247-285.

Cerling, T. E., Hay, R. L., and O'Neil, J. R., 1978, Isotopic, geochemical, and faunal evidence for Pleistocene climatic change in East Africa: Open-File Report 78-701 U. S. Geological Survey, p. 63-65.

Cohen, A. S., 2003, Paleolimnology The History and Evolution of Lake Systems. Oxford University Press, New York, New York, 2003

Crawford, E., W. , and Haynes, J. T., 2002, The chemical character of fluids forming diagenetic illite in the southern Appalachian Basin: American Mineralogist, v. 87, no. 11-12, p. 1519-1527.

Deer, W. A., Howie, R. A., and Zussman, J., 1992, An Introduction to the Rock-Forming Minerals (2nd Edition), p. 353-357.

deMenocal, P. B., 1995, Plio-Pleistocene African Climate: Science, v. 270, no. 5233, p. 53-59.

-, 2011, Climate and Human Evolution: Science, v. 331, p. 540-542.

Deocampo, D. M., 2004, Authigenic clays in East Africa: Regional trends and paleolimnology at the Plio-Pleistocene boundary, Olduvai Gorge, Tanzania: Journal of Paleolimnology, v. 31, p. 1-9.

Deocampo, D. M., Behrensmeyer, A. K., and Potts, R., 2010, Ultrafine Clay Minerals of the Pleistocene Olorgesallie Formation, Southern Kenya Rift: Diagenesis and Paleoenvironments of Early Hominins: Clays and Clay Minerals, v. 58, no. 3, p. 294-310.

Deocampo, D. M., Cuadros, J., Wing-Dudek, T., Olives, J., and Amouric, M., 2009, Saline Lake Diagenesis as Revealed by Coupled Mineralogy and Geochemistry of Multiple Ultrafine Clay Phases: Pliocene Oluvai gorge, Tanzania: American Journal of Science, v. 309.

Deocampo, D. M., Hay, R. L., Ashley, G. M., Kyser, K., and Liutkus, C. M., 2000, Lacustrine clay diagenesis in northern Tanzania, and paleoenvironmental applications at Olduvai Gorge: Abstracts with Programs - Geological Society of America, v. 32, no. 7, p. 366-366.

Eberl, D. D., 1993, Synthesis of Illite-Smectite from Smectite at Earth Surface Temperatures and High pH: Clay Minerals, no. 28, p. 49-60.

Hay, R. L., 1963, Stratigraphy of Beds I through IV, Olduvai gorge, Tanganyika: Science, v. 139, no. 3557, p. 829-833.

Hay, R. L., 1967, Revised stratigraphy of Olduvai gorge, Background to the Evolution in Africa p. 221-228.

Hay, R. L., 1970, Silicate reactions in three lithofacies of a semi-arid basin, Olduvai Gorge, Tanzania: Special Paper - Mineralogical Society of America, v. 3, p. 237-255.

Hay, R. L., 1976a, Geological investigations of Olduvai Gorge, 1968: Research Reports - National Geographic Society, v. 9, p. 163-163.

-, 1976b, Geology of the Olduvai Gorge; a study of sedimentation in a semiarid basin, United States, Univ. Calif. Press : Berkeley, Calif., United States.

Hay, R. L., 1981, Lithofacies and environments of Bed I, Olduvai Gorge, Tanzania: AAAS Selected Symposia Series, v. 63, p. 25-55.

Hay, R. L., and Kyser, T. K., 1996, Hominid-bearing deposits of bed I and lower bed II, Olduvai Gorge; a clay mineral and isotopic contribution: Abstracts with Programs - Geological Society of America, v. 28, no. 6, p. 44-44.

-, 2001, Chemical sedimentology and paleoenvironmental history of Lake Olduvai, a Pliocene lake in northern Tanzania: Geological Society of America Bulletin, v. 113, no. 12, p. 1505-1521.

Hay, R. L., and Kyser, T. K., 2002, Lake Olduvai, a Pliocene lake in northern Tanzania; determining chemistry and evaporative concentration: Abstracts with Programs - Geological Society of America, v. 34, no. 6, p. 293-293.

Hay, R. L., Pexton, R. E., Teague, T. T., and Kyser, T. K., 1986, Spring-related carbonate rocks, Mg Clays and associated minerals in Pliocene deposits of the Amargosa Desert, Nevada and California: Geological Society of America Bulletin, v. 97, p. 1488-1503.

Heiri, O., Lotter, A. F., and Lemke, G., 2001, Loss on ignition as a method for estimating organic and carbonate content in sediments: reproducibility and comparability of results: Journal of Paleolimnology, v. 25, p. 101-110.

Hover, V. C., and Ashley, G. M., 2003, Geochemical signatures of paleodepositional and diagenetic environments: A STEM/AEM study of authigenic clay minerals from an arid rift basin, Olduvai Gorge, Tanzania, v. 51, no. 3, p. 231-251.

Hover, V. C., Ashley, G. M., Driese, S. G., Owen, R. B., and McBrearty, S., 2005, Authigenic Mg-rich smectite and 10-Aa clay minerals in East African Rift-valley lacustrine sediments; what do compositions tell you about geochemical depositional environments?, *in*

Anonymous, Ashley, G. M., Driese, S. G., Owen, R. B., and McBrearty, S., eds., Volume 42: United States, Clay Minerals Society, p. 54-55.

Hover, V. C., Walter, L. M., Peacor, D. R., and Martini, A. M., 1999, Mg-Smectite Authigenesis in a Marine Evaporative Environment, Salina Ometepec. Baja California: Clays and Clay Minerals, v. 47, no. 3, p. 252-268.

Johnson, T. C., Brown, E. T., McManus, J., Barry, S., Barker, P., and Gasse, F., 2002, high-resolution paleoclimate record spanning the past 25,000 years in southern East Africa: Science, v. 296, no. 5565, p. 113-111+.

Jones, B. F., 1986, Clay Mineral Diagenesis in Lacustrine Sediments: Studies in Diagenesis, v. U.S. Geological Survey Bulletin, no. 1578, p. 291-300.

Jones, B. F., and Deocampo, D. M., 2003, Geochemistry of Saline Lakes: Treatise on Geochemistry, v. 5, p. 393-424.

Lanson, B., Sakharov, B. A., Claret, F., and Drits, V. A., 2009, Diagenetic smectite-to-illite transition in clay-rich sediments: A reappraisal of X-ray diffraction results using the multispecimen method: American Journal of Science, v. 309, no. 6, p. 476-516.

Leakey, M. D., 1971, Olduvai Gorge, Volume 3, Excavations in Beds I and II, 1960-1963: London, Cambridge University Press.

Levin, N. E., Quade, J., Simpson, S. W., Semaw, S., and Rogers, M., 2004, Istopic evidence for Plio-Pleistocene environmental change at Gona, Ethiopia Earth and Planetary Science Letters, v. 219, p. 93-110.

Liutkus, C. M., Wright, J. D., Ashley, G. M., and Sikes, N. E., 2005, Paleoenvironmental interpretation of lake-margin deposits using delta C-13 and delta O-18 results from early Pleistocene carbonate rhizoliths, Olduvai Gorge, Tanzania: GEOLOGY, v. 33, no. 5, p. 377-380.

McHenry, L. J., 2009, Element Mobility During Zeolitic and Argillic Alteration of Volcanic Ash in a Closed-basin Lacustrine Environment: Case Study Olduvai Gorge, Tanzania: Chemical Geology, v. 265, p. 540-552.

Renaut, R. W., Tiercelin, J. J., and Owen, R. B., 1986, Mineral Precipitation and Diagenesis in the Sediments of Lake Bogoria Basin, Kenya Rift Valley: in Frostick, L.E. et al., eds., Sedimentation in the African Rifts: Geological Society Special Publications, v. 25, p. 159-175.

Rosen, M. R., 1994, The importance of groundwater in playas: A review of playa classifications and the sedimentology and hydrology of playas: Geological Society of America Special Papers, v. 289.

Santisteban, J. I., Mediavilla, R., Lopez-Pamo, E., Dabrio, C. J., Zapata, M. B. R., Garcia, M. J. G. G., Castano, S., and Martinez-Alfaro, P. E., 2004, Loss on ignition: a qualitative or quantitative method for organic matter and carbonate mineral content in sediments: Journal of Paleolimnology, v. 32, p. 287-299.

Singer, A., and Stoffers, P., 1980, Clay mineral diagenesis in two East African lake sediments: Clay Minerals, v. 15, no. 3, p. 291-307.

Trauth, M. H., Larrasonana, J. C., and Mudelsee, M., 2009, Trends, rhythms and events in Plio-Pleistocen African climate: Quaternary Science Reviews, v. 28, p. 399-411.

Trauth, M. H., Maslin, M., Deino, A. L., and Strecker, M. R., 2005, Late Cenozoic Moisture History of East Africa: Science, v. 309, p. 2051-2053.

Trauth, M. H., Maslin, M. A., Deino, A. L., Strecker, M. R., Bergner, A. G. N., and Duhnforth, M., 2007, High- and low- latitude forcing of Plio-Pleistocene East African climate and human evolution: Journal of Human Evolution, v. 53, p. 475-486.

Tuenter, E., Weber, S. L., Hilgen, F. J., and Lourens, L. J., 2003, The response of the African summer monsoon to remote and local forcing due to precession an dobliquity: Global and Planetary Change, v. 36, p. 219-235.

U.S. Department of the Interior, U. S. G. S., 2001a, A Laboratory Manual for X-Ray Powder Dffraction Smectite Group: U.S. Geological Survey Open-File Report 01-041.

-, 2001b, A Laboratory Manual for X-Ray Powder Diffraction Illite Group: U.S. Geological Survey Open-File Report 01-041.

Webster, D. M. a. Jones, B.F., 1994, Paleoenvironmental Implications of Lacustrine Clay Minerals from the Double Lakes Formation, Southern High Plains, Texas: Sedimentology and Geochemistry of Modern and Ancient Saline Lakes, v. SEPM Special Publication, no. 50, p. 159-172.

Yuretich, R., Long, D. T., and Giesy, J. P., 1995, Clay minerals in lake sediments as proxies for environmental change, *in* Long, D. T., and Giesy, J. P., eds., Volume 38: International, International Association for Great Lakes Research (IAGLR).

Yuretich, R. F., and Cerling, T. E., 1983, Hydrogeochemistry of Lake Turkana, Kenya; mass balance and mineral reactions in an alkaline lake: Geochimica Et Cosmochimica Acta, v. 47, no. 6, p. 1099-1109.

Yuretich, R. F., Frostick, L. E., Renaut, R. W., Reid, I., and Tiercelin, J. J., 1986, Controls on the composition of modern sediments, Lake Turkana, Kenya, *in* Frostick, L. E., Renaut, R. W., Reid, I., and Tiercelin, J. J., eds., Volume 25: United Kingdom, Geological Society of London, p. 141-152.

Yuretich, R. F., Renaut, R. W., Ervin, C. R., and Ashley, G. M., 2002, Clay minerals as paleoenvironmental indicators in two large lakes of the African rift valleys; Lake Malawi and Lake Turkana: Special Publication - Society for Sedimentary Geology, v. 73, p. 221-232.

7. APPENDICES

Appendix A: Major Element Oxide data from XRF analysis and LOI

*Sample lithology is claystone unless otherwise noted: CN=chert nodules in claystone, T=tuff/inclusion of tuff, D=dolostone/dolomite, C=presence of calcite

Sample ID	Depth from Bottom	Elements Present in Weight Percent										Total Wt%	LOI_{550}	LOI_{950}	Total Wt % + LOI
GAL	Meters	SiO_2	TiO_2	Al_2O_3	Fe_2O_3	MnO	MgO	CaO	Na_2O	K_2O	P_2O_5	%	%	%	%
179	34.05	67.98	0.87	11.73	3.55	0.06	2.15	5.60	3.22	2.96	0.12	98.24			
178	33.40	53.40	0.63	7.77	2.71	0.09	1.62	18.75	2.15	2.31	0.16	89.59			
177	32.90	48.97	1.87	11.85	9.64	0.17	6.28	4.41	2.93	4.78	0.18	91.08			
176	32.00	44.67	1.59	10.86	8.80	0.16	5.14	10.76	2.74	4.25	0.19	89.16			
174-T	31.90	39.95	1.02	9.67	8.05	0.18	4.69	17.30	3.92	2.97	0.10	87.85			
175	31.70	50.11	1.93	12.22	9.94	0.19	5.60	3.88	3.48	4.71	0.20	92.26			
173	31.30	45.05	1.45	9.31	7.08	0.11	5.27	9.73	2.54	3.80	0.21	84.55			
172	31.00	38.05	1.17	7.81	6.04	0.10	3.53	18.88	2.19	3.10	0.16	81.03			
171	30.20	48.88	0.77	7.45	2.73	0.09	3.12	20.29	1.87	1.80	0.15	87.15			
170	30.10	42.44	0.44	4.19	1.94	0.12	2.14	27.16	0.90	1.45	0.11	80.89			
169	30.05	49.92	1.08	6.22	4.80	0.20	3.65	19.40	1.17	3.73	0.37	90.54			
168	29.95	47.46	1.36	9.29	7.22	0.16	4.22	11.00	1.67	7.41	0.52	90.31			
166	29.85	54.28	1.47	8.79	7.35	0.11	4.57	5.33	2.02	6.47	0.25	90.64			
165	29.55	50.90	1.27	8.85	6.25	0.10	5.29	8.77	1.79	7.44	0.42	91.08			
167	29.50														
164	29.40	52.49	1.14	7.94	5.51	0.13	7.41	9.47	1.91	6.84	0.43	93.27			
163-C	29.20	32.48	0.78	5.00	3.87	0.28	3.50	28.28	0.92	3.14	0.17	78.42			
162	29.15	53.02	1.23	8.18	6.38	0.15	5.48	9.31	1.50	6.10	0.33	91.68			
161	29.10	43.04	1.05	7.43	6.70	0.17	4.89	15.54	1.15	5.84	0.17	85.98			
160	29.00	40.79	1.09	7.91	5.66	0.22	4.71	18.24	0.85	6.71	0.14	86.32			

Sample ID	Depth from Bottom	Elements Present in Weight Percent										Total Wt%	LOI_{550}	LOI_{950}	Total Wt % + LOI
GAL	Meters	SiO_2	TiO_2	Al_2O_3	Fe_2O_3	MnO	MgO	CaO	Na_2O	K_2O	P_2O_5	%	%	%	%
159	28.80	45.38	1.27	8.12	10.10	0.15	6.06	12.73	1.01	6.48	0.27	91.57			
158	28.70														
157-C	28.20	28.94	0.72	5.19	4.50	0.10	3.69	29.38	0.95	4.72	0.12	78.31			
156	28.10	55.44	1.34	9.24	6.74	0.16	9.34	2.67	1.87	8.70	0.11	95.61			
155	27.95														
154-C	27.55	52.19	0.55	9.77	4.99	0.10	7.74	6.42	1.46	7.26	0.07	90.55			
153	27.50	53.05	0.84	13.12	6.92	0.09	2.51	4.85	4.19	5.54	0.12	91.23			
152	27.20														
151	27.10	60.43	0.66	15.82	5.23	0.09	1.80	2.57	3.17	9.07	0.10	98.94			
36-D	27.05	12.28	0.42	2.23	1.69	0.51	24.20	27.35	0.33	1.49	0.05	70.55			
37	27.00	38.00	0.67	5.42	4.34	0.10	9.71	17.39	1.56	4.14	0.11	81.44	8.00	13.00	102
38	26.80	48.35	1.10	7.86	5.42	0.15	9.57	10.54	1.80	5.88	0.15	90.82	9.00	7.00	107
39	26.75	39.16	0.57	6.40	7.07	0.09	7.05	17.19	1.75	4.71	0.08	84.07	8.00	13.00	105
40	26.70	27.21	0.49	4.84	3.87	0.08	5.42	31.97	1.15	3.90	0.07	79.00	4.00	23.00	106
41	26.35														
42	26.15	31.11	0.62	5.88	3.69	0.16	7.44	25.10	1.85	3.33	0.15	79.33	6.00	19.00	104
43	26.05	43.78	0.82	8.15	5.47	0.13	9.18	10.25	2.81	4.04	0.22	84.85	8.00	9.00	102
44	25.95	43.79	1.05	9.27	5.85	0.17	8.33	11.68	2.94	5.15	0.12	88.35			
45	25.85	45.52	0.80	10.35	6.28	0.17	5.72	9.90	3.79	4.73	0.14	87.4	8.00	8.00	103
46	25.70	45.11	0.88	6.81	5.79	0.11	13.18	8.45	2.05	4.99	0.10	87.47	11.00	6.00	104
47	25.60	45.31	0.90	7.05	6.06	0.15	12.69	8.82	1.99	5.13	0.11	88.21			
48	25.20	49.08	0.83	7.40	4.65	0.14	11.58	7.52	1.87	6.63	0.17	89.87	9.00	6.00	105
49	25.05	48.98	0.87	7.50	4.30	0.12	10.18	7.07	2.03	5.68	0.14	86.87			
50	24.95	53.61	0.75	11.17	8.84	0.10	6.41	2.41	1.94	8.70	0.09	94.02	8.00	2.00	104
51	24.70	51.55	1.11	9.88	5.40	0.15	8.21	4.94	2.48	6.83	0.12	90.67			

Sample ID	Depth from Bottom	Elements Present in Weight Percent										Total Wt%	LOI_{550}	LOI_{950}	Total Wt % + LOI
GAL	Meters	SiO_2	TiO_2	Al_2O_3	Fe_2O_3	MnO	MgO	CaO	Na_2O	K_2O	P_2O_5	%	%	%	%
52-T	24.55	55.77	0.80	12.42	4.94	0.10	2.30	11.11	3.53	5.87	0.16	97.00			
53-T	24.40	50.85	1.25	9.54	4.25	0.15	7.68	7.06	2.72	7.85	0.13	91.48			
54-T	24.30	55.33	0.65	16.61	6.12	0.03	0.90	1.46	5.47	6.63	0.07	93.27	8.00	1.00	102
55-T	24.20	53.63	0.79	11.76	6.09	0.14	5.91	5.00	2.18	8.97	0.13	94.6			
56	24.10	48.57	0.88	8.27	4.24	0.14	9.63	8.85	2.31	6.16	0.12	89.17	8.00	7.00	104
57-T	24.05	53.56	0.90	13.22	8.66	0.10	4.22	3.00	3.96	6.15	0.15	93.92	10.00	2.00	106
58	23.95	44.59	0.73	6.75	4.55	0.13	11.98	8.38	2.53	4.59	0.14	84.37			
59	23.90	49.65	0.86	8.36	5.85	0.16	10.81	4.43	2.60	4.84	0.13	87.69			
60	23.80	49.88	0.98	9.60	6.04	0.16	8.50	6.47	2.93	5.86	0.13	90.55	9.00	5.00	105
61-T	23.50	54.86	0.78	13.24	6.37	0.13	4.71	2.06	4.34	5.71	0.14	92.34			
62	23.30	53.03	0.63	9.92	4.77	0.14	10.83	4.80	2.00	7.01	0.10	93.23	8.00	4.00	105
63	23.05	47.40	1.10	8.64	5.98	0.15	10.88	4.79	3.52	5.49	0.15	88.1			
64-T	22.80	51.86	0.85	11.24	6.21	0.12	5.19	5.12	2.63	7.39	0.13	90.74			
65	22.60	54.85	1.14	11.25	7.54	0.19	8.61	4.57	2.46	7.85	0.12	98.58			
66	22.50	51.05	1.05	10.33	6.55	0.12	7.14	4.13	2.45	7.11	0.12	90.05			
68	21.80	44.89	0.88	8.13	5.63	0.15	7.50	10.60	2.34	4.87	0.14	85.13			
67-T	21.73	56.43	0.73	14.53	5.86	0.04	1.88	0.83	4.87	6.27	0.07	91.51			
69	21.70	48.54	1.09	9.20	5.85	0.11	7.64	6.79	2.81	5.16	0.16	87.35			
70	21.40	48.13	0.99	9.04	5.62	0.11	8.70	8.47	2.12	5.12	0.12	88.42			
71	21.00	48.27	1.05	9.28	6.59	0.11	8.23	6.34	2.17	5.63	0.14	87.81			
72	20.95	36.34	0.57	4.42	3.07	0.14	16.62	13.09	1.55	2.62	0.09	78.51	8.00	17.00	104
73	20.90	43.54	0.68	5.35	4.04	0.09	17.21	6.16	1.98	3.69	0.08	82.82	11.00	9.00	103
149	20.30	49.94	1.06	8.72	6.36	0.20	12.28	3.98	2.54	5.83	0.09	91			
148	20.10	55.23	0.88	12.24	6.76	0.17	6.18	3.74	2.57	8.28	0.10	96.15			
147	20.05	53.16	0.86	11.58	5.52	0.13	6.14	5.40	2.59	8.44	0.10	93.92			

Sample ID	Depth from Bottom	Elements Present in Weight Percent										Total Wt%	LOI_{550}	LOI_{950}	Total Wt % + LOI
GAL	Meters	SiO_2	TiO_2	Al_2O_3	Fe_2O_3	MnO	MgO	CaO	Na_2O	K_2O	P_2O_5	%	%	%	%
146	19.95	52.71	0.85	10.13	6.96	0.14	9.08	4.49	1.91	7.44	0.09	93.8			
145-T	19.80	62.06	0.82	16.00	4.08	0.03	1.49	0.62	5.89	6.66	0.05	97.7			
144	19.30														
143	19.10	46.01	0.80	8.96	5.41	0.10	9.32	9.06	2.26	5.64	0.08	87.64			
142	18.95	44.75	0.83	9.14	5.23	0.16	12.61	7.94	1.81	5.84	0.12	88.43			
141	18.60	37.65	0.59	7.11	4.01	0.14	12.01	13.86	1.57	4.53	0.18	81.65			
140	18.30	44.17	0.73	8.99	4.84	0.15	10.74	8.53	2.62	5.78	0.08	86.63			
139	18.00	52.54	0.67	8.94	4.72	0.09	11.37	5.55	2.55	5.36	0.07	91.86			
137-C	17.85	38.68	0.51	5.57	3.33	0.14	9.91	16.17	1.82	3.39	0.07	79.59			
136-C	17.15	25.21	0.36	4.32	1.93	0.15	6.28	30.91	1.43	2.73	0.05	73.37			
135	17.10	50.74	0.76	6.77	6.27	0.08	15.08	3.21	2.59	4.66	0.06	90.22			
105	16.95	42.38	0.56	7.73	4.11	0.11	8.08	13.84	3.17	4.86	0.07	84.91			
104-T	16.70	48.69	0.30	11.63	4.25	0.08	2.91	11.49	3.75	5.86	0.08	89.04			
103	16.50	41.66	0.70	8.24	4.18	0.13	6.03	16.13	2.64	5.31	0.14	85.16			
102	16.15	52.84	1.02	10.15	5.65	0.14	8.80	6.62	3.01	7.14	0.12	95.49			
101-C	16.05	35.46	0.71	6.15	3.79	0.29	6.50	20.01	1.56	4.06	0.09	78.62			
99	16.00	52.29	1.01	10.53	6.59	0.18	6.87	5.68	2.42	6.81	0.11	92.49			
100-T	16.00	47.46	0.89	9.05	8.05	0.18	6.75	8.52	1.91	6.52	0.13	89.46			
98	15.95														
97	15.90	50.13	0.65	11.07	6.51	0.16	4.37	5.59	2.92	6.61	0.11	88.12			
96	15.85	50.47	1.07	9.22	6.24	0.16	8.46	7.21	2.12	6.59	0.12	91.66			
95	15.70	54.44	0.45	13.17	5.69	0.09	2.87	5.85	3.24	7.39	0.14	93.33			
94	15.60	47.17	0.88	7.67	4.98	0.12	9.46	8.25	2.55	5.65	0.13	86.86			
92	15.05	35.90	0.91	7.32	8.99	0.07	4.45	12.69	1.75	5.46	0.09	77.63			
91	15.00	35.04	0.67	5.23	3.28	0.13	8.14	19.82	2.30	3.77	0.12	78.5			
90	14.80	46.48	0.79	6.92	3.70	0.10	10.44	9.64	2.66	4.64	0.14	85.51	9.00	7.00	102

Sample ID	Depth from Bottom	Elements Present in Weight Percent										Total Wt%	LOI_{550}	LOI_{950}	Total Wt % + LOI
GAL	Meters	SiO_2	TiO_2	Al_2O_3	Fe_2O_3	MnO	MgO	CaO	Na_2O	K_2O	P_2O_5	%	%	%	%
89	14.55	41.61	0.66	5.61	3.87	0.10	9.88	14.58	1.94	4.80	0.17	83.22	9.00	10.00	102
88	14.40	49.23	0.59	4.12	3.43	0.12	16.95	5.42	2.45	3.72	0.12	86.15	14.00	4.00	104
87-CN	14.30	49.27	0.59	4.05	3.26	0.09	17.76	6.10	2.75	3.59	0.14	87.6	16.00	5.00	109
86	14.24	36.52	0.47	3.43	2.56	0.08	11.69	17.66	2.50	2.83	0.07	77.81	13.00	11.00	102
85-T	14.20	45.15	0.49	11.55	8.66	0.08	4.98	9.51	2.78	6.84	0.12	90.16			
84	14.15	37.12	0.59	4.60	3.39	0.07	10.65	15.50	2.14	3.40	0.11	77.57			
93	14.15	47.35	0.90	6.78	4.57	0.11	11.23	8.64	2.10	5.18	0.19	87.05			
83-C	14.10	28.35	0.43	3.32	2.42	0.06	8.13	20.62	2.20	2.67	0.08	68.28			
82	14.05												6.00	10.00	
80-C	13.95	27.99	0.44	2.84	2.62	0.07	10.58	17.97	3.27	2.56	0.04	68.38	12.00	15.00	95
81	13.90	40.75	0.59	4.91	4.31	0.08	13.97	8.25	3.27	4.20	0.05	80.38	13.00	6.00	99
79	13.70	39.21	0.50	3.62	2.77	0.05	17.30	10.61	3.36	2.30	0.05	79.77	13.00	10.00	103
78	13.60	44.06	0.61	5.96	3.98	0.08	13.66	7.96	2.86	4.60	0.06	83.83	11.00	7.00	102
77	13.50	31.11	0.44	3.26	2.72	0.06	14.30	16.19	2.72	2.09	0.06	72.95			
76	13.45	42.26	0.57	4.07	3.23	0.06	17.90	7.42	3.44	2.92	0.05	81.92	15.00	7.00	104
75-C	13.40	37.76	0.54	3.73	3.01	0.08	16.44	17.18	3.06	3.07	0.05	84.92	11.00	14.00	110
74-C	13.15	41.84	0.57	4.57	3.55	0.07	16.61	10.52	2.57	3.11	0.07	83.48	13.00	8.00	104
134-C	12.80	43.31	0.46	3.94	3.26	0.05	16.33	8.67	2.38	2.85	0.07	81.32			
133-D	12.30	18.04	0.43	3.11	2.52	0.16	20.59	19.79	1.34	2.13	0.12	68.23			
132-D	12.05	26.44	0.54	4.06	2.98	0.13	19.58	15.02	1.58	2.96	0.08	73.37			
131	11.95														
130	11.85	44.59	0.77	5.75	3.78	0.08	13.40	8.31	2.42	3.89	0.08	83.07			
129	11.70	43.11	0.81	7.01	5.36	0.13	7.67	10.20	2.37	5.67	0.10	82.43			
128	11.30	40.83	0.64	9.02	11.06	0.07	3.46	6.91	2.92	6.06	0.16	81.13			
127	11.15	54.88	1.32	9.71	6.65	0.10	10.42	2.02	3.41	7.81	0.10	96.42	10.00	2.00	108
126	11.05	46.38	0.77	10.08	7.44	0.10	4.72	6.49	2.89	7.55	0.18	86.6	8.00	3.00	98

Sample ID	Depth from Bottom	Elements Present in Weight Percent										Total Wt%	LOI_{550}	LOI_{950}	Total Wt % + LOI
GAL	Meters	SiO_2	TiO_2	Al_2O_3	Fe_2O_3	MnO	MgO	CaO	Na_2O	K_2O	P_2O_5	%	%	%	%
125	10.95	45.92	0.76	5.89	4.12	0.07	12.22	6.91	3.40	4.40	0.09	83.78			
124-T	10.90	16.52	0.25	2.30	7.67	0.04	2.90	26.50	1.74	1.70	0.06	59.68	9.00	17.00	86
123	10.80	42.63	0.73	5.58	4.09	0.08	11.55	9.04	4.41	4.38	0.09	82.58			
122-C	10.30	45.46	0.77	5.93	4.37	0.08	12.09	8.78	3.27	4.42	0.09	85.26			
121	10.05	48.67	0.88	6.75	4.77	0.07	11.82	5.62	2.86	4.90	0.08	86.42	11.00	4.00	101
120	9.95	42.42	0.85	7.13	4.92	0.09	7.71	11.94	3.45	5.10	0.17	83.78	9.00	8.00	101
119	9.70	43.48	0.69	5.72	4.28	0.08	11.62	10.94	2.88	4.46	0.11	84.26	11.00	8.00	103
118	9.55	43.98	0.74	5.76	4.15	0.09	11.97	10.25	2.95	4.40	0.12	84.41			
117-T	9.45	37.09	0.78	6.41	5.77	0.09	6.38	11.43	2.46	4.54	0.14	75.09	12.00	4.00	91
116	9.10	48.77	1.01	7.57	5.63	0.07	11.09	5.21	3.16	5.80	0.14	88.45			
115	9.00	40.71	0.71	5.10	3.76	0.09	12.25	11.61	3.66	3.62	0.07	81.58			
114	8.90	39.73	0.55	4.58	3.55	0.07	13.53	9.39	3.73	3.13	0.08	78.34			
113-T	8.80	34.72	0.45	3.48	2.79	0.13	17.47	10.60	5.03	2.35	0.06	77.08			
112	8.50	40.28	0.58	4.51	3.39	0.07	15.47	8.80	4.99	3.26	0.06	81.41	13.00	7.00	101
111	8.30	36.19	0.58	4.51	3.13	0.08	18.85	9.13	3.11	3.13	0.07	78.78			
110	8.10	46.28	0.75	5.68	3.99	0.07	17.43	2.83	3.74	3.82	0.08	84.67			
109	8.00	25.97	0.54	4.23	3.44	0.08	15.47	11.91	6.73	2.84	0.06	71.27			
108	7.85														
107	7.55	33.73	0.70	5.16	3.67	0.08	21.27	12.27	3.32	3.80	0.05	84.05			
106	7.40	33.01	0.65	4.84	3.56	0.08	19.90	11.40	3.34	3.63	0.06	80.47			
35	7.00	36.06	0.69	5.26	3.52	0.08	18.87	9.80	2.53	3.65	0.07	80.53	19.00	6.00	106
34	6.90	25.08	0.45	3.26	2.70	0.06	21.16	15.97	1.87	2.38	0.04	72.97			
33	6.60	28.36	0.49	3.56	2.73	0.06	21.77	14.50	1.29	2.48	0.05	75.29			
32	6.30	18.52	0.32	2.74	2.41	0.08	21.51	19.71	2.87	1.97	0.14	70.27	23.00	12.00	105
31	6.05	41.99	0.62	5.00	3.81	0.06	19.94	3.87	4.10	3.24	0.07	82.7	18.00	4.00	105
30-C	6.00	33.82	0.61	4.80	3.45	0.06	11.93	13.25	4.45	3.36	0.06	75.79	12.00	9.00	97

Sample ID	Depth from Bottom	Elements Present in Weight Percent										Total Wt%	LOI_{550}	LOI_{950}	Total Wt % + LOI
GAL	Meters	SiO_2	TiO_2	Al_2O_3	Fe_2O_3	MnO	MgO	CaO	Na_2O	K_2O	P_2O_5	%	%	%	%
29-C	5.80	29.50	0.59	4.66	3.62	0.07	10.44	23.76	3.29	3.44	0.06	79.43	9.00	16.00	104
28-C	5.60	37.38	0.71	5.57	4.05	0.06	11.13	10.44	4.41	3.94	0.06	77.75			
27	5.40	32.68	0.71	5.43	3.72	0.07	12.08	13.70	4.41	4.02	0.06	76.88			
26	5.05	26.96	0.64	4.78	3.58	0.08	17.60	14.83	3.59	3.89	0.07	76.02	21.00	8.00	105
25	5.00	34.29	0.46	9.61	8.99	0.03	3.89	9.08	5.19	5.21	0.12	76.87	12.00	3.00	92
24-T	4.95	22.98	0.41	2.63	1.99	0.07	21.04	15.87	3.53	2.01	0.06	70.59	22.00	11.00	104
23	4.60	32.32	0.51	3.90	2.76	0.08	20.74	11.95	3.22	2.99	0.08	78.55	21.00	7.00	107
22	4.20	31.80	0.52	3.13	2.44	0.08	21.01	11.84	2.65	2.30	0.08	75.85			
21	4.10	31.16	0.28	2.18	1.73	0.04	13.74	20.71	3.03	1.59	0.04	74.50	14.00	16.00	105
20	4.00	28.06	0.44	4.46	3.11	0.06	7.17	19.61	4.54	3.65	0.06	71.16	8.00	14.00	93
19-T	3.80	38.18	0.87	6.99	5.32	0.07	9.01	15.43	2.32	3.65	0.15	81.99			
18-T	3.60	36.73	0.76	7.85	5.90	0.12	13.11	10.27	4.56	2.32	0.05	81.67	12.00	11.00	105
17-T	3.40	38.50	1.19	8.41	6.25	0.12	10.15	13.52	3.48	2.83	0.08	84.53	10.00	12.00	107
16-T	3.20	33.73	0.78	7.69	5.59	0.12	8.16	19.21	2.64	2.99	0.16	81.07			
15	3.00	43.76	1.01	5.86	4.00	0.10	15.02	10.06	2.57	2.86	0.11	85.35			
14	2.80	41.57	0.91	5.65	4.12	0.18	14.42	10.45	2.77	2.61	0.10	82.78	15.00	8.00	106
13	2.60	51.16	1.01	8.09	4.94	0.07	14.82	3.15	3.43	3.41	0.12	90.2	14.00	3.00	107
12	2.40	43.66	0.72	5.01	3.86	0.11	16.36	9.00	2.92	2.43	0.11	84.18	15.00	7.00	106
11	2.20	44.23	0.82	6.61	4.32	0.09	14.91	10.81	3.78	2.82	0.10	88.49	15.00	8.00	111
10	2.00	53.96	1.40	10.61	7.31	0.17	8.76	3.56	2.46	5.38	0.13	93.74			
9	1.80	48.86	1.31	11.00	7.00	0.26	3.37	8.23	3.11	5.24	0.32	88.7			
8	1.60	54.06	1.43	12.41	9.27	0.34	5.16	1.71	2.21	6.77	0.40	93.76			
7	1.40	52.66	1.36	11.73	8.84	0.72	4.98	2.63	2.35	6.04	0.50	91.81			
6	1.20	46.00	1.20	10.70	8.31	1.38	3.94	8.28	2.77	5.67	0.64	88.89			
5-T	1.00	51.32	1.21	11.91	7.98	0.27	3.21	4.96	4.56	5.20	0.27	90.89			
4-T	0.75	54.89	1.31	12.89	7.75	0.12	3.32	4.66	5.58	5.31	0.25	96.08			

Sample ID	Depth from Bottom	Elements Present in Weight Percent										Total Wt%	LOI_{550}	LOI_{950}	Total Wt % + LOI
GAL	Meters	SiO_2	TiO_2	Al_2O_3	Fe_2O_3	MnO	MgO	CaO	Na_2O	K_2O	P_2O_5	%	%	%	%
3-T	0.50	44.10	1.02	10.60	6.47	0.44	2.17	12.57	4.82	3.98	0.38	86.55			
2-T	0.25	58.96	1.17	14.22	7.52	0.08	2.01	1.87	7.07	5.14	0.28	98.32			
1-T	0.00	56.15	1.28	13.45	7.89	0.08	1.73	1.82	6.01	4.66	0.31	93.38			

Appendix B: Normalized Major Element Oxide data from XRF analysis and Oxide Ratios.

*Sample lithology is claystone unless otherwise noted: CN=chert nodules in claystone, T=tuff/inclusion of tuff, D=dolostone/dolomite, C=presence of calcite

Sample ID	Depth from Bottom	Elements Present in Weight Percent: Normalized Data											Ratios	
GAL	Meters	SiO_2	TiO_2	Al_2O_3	Fe_2O_3	MnO	MgO	CaO	Na_2O	K_2O	P_2O_5	Total	Al_2O_3/ MgO	K_2O/ MgO
179	34.05	69.20	0.89	11.94	3.61	0.06	2.19	5.70	3.28	3.01	0.12	100.00	5.46	1.38
178	33.40	59.60	0.70	8.67	3.02	0.10	1.81	20.93	2.40	2.58	0.18	100.00	4.80	1.43
177	32.90	53.77	2.05	13.01	10.58	0.19	6.90	4.84	3.22	5.25	0.20	100.00	1.89	0.76
176	32.00	50.10	1.78	12.18	9.87	0.18	5.76	12.07	3.07	4.77	0.21	100.00	2.11	0.83
174-T	31.90	45.48	1.16	11.01	9.16	0.20	5.34	19.69	4.46	3.38	0.11	100.00	2.06	0.63
175	31.70	54.31	2.09	13.25	10.77	0.21	6.07	4.21	3.77	5.11	0.22	100.00	2.18	0.84
173	31.30	53.28	1.71	11.01	8.37	0.13	6.23	11.51	3.00	4.49	0.25	100.00	1.77	0.72
172	31.00	46.96	1.44	9.64	7.45	0.12	4.36	23.30	2.70	3.83	0.20	100.00	2.21	0.88
171	30.20	56.09	0.88	8.55	3.13	0.10	3.58	23.28	2.15	2.07	0.17	100.00	2.39	0.58
170	30.10	52.47	0.54	5.18	2.40	0.15	2.65	33.58	1.11	1.79	0.14	100.00	1.96	0.68
169	30.05	55.14	1.19	6.87	5.30	0.22	4.03	21.43	1.29	4.12	0.41	100.00	1.70	1.02
168	29.95	52.55	1.51	10.29	7.99	0.18	4.67	12.18	1.85	8.21	0.58	100.00	2.20	1.76
166	29.85	59.89	1.62	9.70	8.11	0.12	5.04	5.88	2.23	7.14	0.28	100.00	1.92	1.42
165	29.55	55.88	1.39	9.72	6.86	0.11	5.81	9.63	1.97	8.17	0.46	100.00	1.67	1.41
167	29.50													
164	29.40	56.28	1.22	8.51	5.91	0.14	7.94	10.15	2.05	7.33	0.46	100.00	1.07	0.92
163-C	29.20	41.42	0.99	6.38	4.93	0.36	4.46	36.06	1.17	4.00	0.22	100.00	1.43	0.90
162	29.15	57.83	1.34	8.92	6.96	0.16	5.98	10.15	1.64	6.65	0.36	100.00	1.49	1.11
161	29.10	50.06	1.22	8.64	7.79	0.20	5.69	18.07	1.34	6.79	0.20	100.00	1.52	1.19
160	29.00	47.25	1.26	9.16	6.56	0.25	5.46	21.13	0.98	7.77	0.16	100.00	1.68	1.42
159	28.80	49.56	1.39	8.87	11.03	0.16	6.62	13.90	1.10	7.08	0.29	100.00	1.34	1.07

Sample ID	Depth from Bottom	Elements Present in Weight Percent: Normalized Data											Ratios	
GAL	Meters	SiO_2	TiO_2	Al_2O_3	Fe_2O_3	MnO	MgO	CaO	Na_2O	K_2O	P_2O_5	Total	Al_2O_3/ MgO	K_2O/ MgO
158	28.70													
157-C	28.20	36.96	0.92	6.63	5.75	0.13	4.71	37.52	1.21	6.03	0.15	100.00	1.41	1.28
156	28.10	57.99	1.40	9.66	7.05	0.17	9.77	2.79	1.96	9.10	0.12	100.00	0.99	0.93
155	27.95													
154-C	27.55	57.64	0.61	10.79	5.51	0.11	8.55	7.09	1.61	8.02	0.08	100.00	1.26	0.94
153	27.50	58.15	0.92	14.38	7.59	0.10	2.75	5.32	4.59	6.07	0.13	100.00	5.23	2.21
152	27.20													
151	27.10	61.08	0.67	15.99	5.29	0.09	1.82	2.60	3.20	9.17	0.10	100.00	8.79	5.04
36-D	27.05	17.41	0.60	3.16	2.40	0.72	34.30	38.77	0.47	2.11	0.07	100.00	0.09	0.06
37	27.00	46.66	0.82	6.66	5.33	0.12	11.92	21.35	1.92	5.08	0.14	100.00	0.56	0.43
38	26.80	53.24	1.21	8.65	5.97	0.17	10.54	11.61	1.98	6.47	0.17	100.00	0.82	0.61
39	26.75	46.58	0.68	7.61	8.41	0.11	8.39	20.45	2.08	5.60	0.10	100.00	0.91	0.67
40	26.70	34.44	0.62	6.13	4.90	0.10	6.86	40.47	1.46	4.94	0.09	100.00	0.89	0.72
41	26.35													
42	26.15	39.22	0.78	7.41	4.65	0.20	9.38	31.64	2.33	4.20	0.19	100.00	0.79	0.45
43	26.05	51.60	0.97	9.61	6.45	0.15	10.82	12.08	3.31	4.76	0.26	100.00	0.89	0.44
44	25.95	49.56	1.19	10.49	6.62	0.19	9.43	13.22	3.33	5.83	0.14	100.00	1.11	0.62
45	25.85	52.08	0.92	11.84	7.19	0.19	6.54	11.33	4.34	5.41	0.16	100.00	1.81	0.83
46	25.70	51.57	1.01	7.79	6.62	0.13	15.07	9.66	2.34	5.70	0.11	100.00	0.52	0.38
47	25.60	51.37	1.02	7.99	6.87	0.17	14.39	10.00	2.26	5.82	0.12	100.00	0.56	0.40
48	25.20	54.61	0.92	8.23	5.17	0.16	12.89	8.37	2.08	7.38	0.19	100.00	0.64	0.57
49	25.05	56.38	1.00	8.63	4.95	0.14	11.72	8.14	2.34	6.54	0.16	100.00	0.74	0.56
50	24.95	57.02	0.80	11.88	9.40	0.11	6.82	2.56	2.06	9.25	0.10	100.00	1.74	1.36
51	24.70	56.85	1.22	10.90	5.96	0.17	9.05	5.45	2.74	7.53	0.13	100.00	1.20	0.83
52-T	24.55	57.49	0.82	12.80	5.09	0.10	2.37	11.45	3.64	6.05	0.16	100.00	5.40	2.55

Sample ID	Depth from Bottom	Elements Present in Weight Percent: Normalized Data											Ratios	
GAL	Meters	SiO_2	TiO_2	Al_2O_3	Fe_2O_3	MnO	MgO	CaO	Na_2O	K_2O	P_2O_5	Total	Al_2O_3/ MgO	K_2O/ MgO
53-T	24.40	55.59	1.37	10.43	4.65	0.16	8.40	7.72	2.97	8.58	0.14	100.00	1.24	1.02
54-T	24.30	59.32	0.70	17.81	6.56	0.03	0.96	1.57	5.86	7.11	0.08	100.00	18.46	7.37
55-T	24.20	56.69	0.84	12.43	6.44	0.15	6.25	5.29	2.30	9.48	0.14	100.00	1.99	1.52
56	24.10	54.47	0.99	9.27	4.75	0.16	10.80	9.92	2.59	6.91	0.13	100.00	0.86	0.64
57-T	24.05	57.03	0.96	14.08	9.22	0.11	4.49	3.19	4.22	6.55	0.16	100.00	3.13	1.46
58	23.95	52.85	0.87	8.00	5.39	0.15	14.20	9.93	3.00	5.44	0.17	100.00	0.56	0.38
59	23.90	56.62	0.98	9.53	6.67	0.18	12.33	5.05	2.96	5.52	0.15	100.00	0.77	0.45
60	23.80	55.09	1.08	10.60	6.67	0.18	9.39	7.15	3.24	6.47	0.14	100.00	1.13	0.69
61-T	23.50	59.41	0.84	14.34	6.90	0.14	5.10	2.23	4.70	6.18	0.15	100.00	2.81	1.21
62	23.30	56.88	0.68	10.64	5.12	0.15	11.62	5.15	2.15	7.52	0.11	100.00	0.92	0.65
63	23.05	53.80	1.25	9.81	6.79	0.17	12.35	5.44	4.00	6.23	0.17	100.00	0.79	0.50
64-T	22.80	57.15	0.94	12.39	6.84	0.13	5.72	5.64	2.90	8.14	0.14	100.00	2.17	1.42
65	22.60	55.64	1.16	11.41	7.65	0.19	8.73	4.64	2.50	7.96	0.12	100.00	1.31	0.91
66	22.50	56.69	1.17	11.47	7.27	0.13	7.93	4.59	2.72	7.90	0.13	100.00	1.45	1.00
68	21.80	52.73	1.03	9.55	6.61	0.18	8.81	12.45	2.75	5.72	0.16	100.00	1.08	0.65
67-T	21.73	61.67	0.80	15.88	6.40	0.04	2.05	0.91	5.32	6.85	0.08	100.00	7.73	3.34
69	21.70	55.57	1.25	10.53	6.70	0.13	8.75	7.77	3.22	5.91	0.18	100.00	1.20	0.68
70	21.40	54.43	1.12	10.22	6.36	0.12	9.84	9.58	2.40	5.79	0.14	100.00	1.04	0.59
71	21.00	54.97	1.20	10.57	7.50	0.13	9.37	7.22	2.47	6.41	0.16	100.00	1.13	0.68
72	20.95	46.29	0.73	5.63	3.91	0.18	21.17	16.67	1.97	3.34	0.11	100.00	0.27	0.16
73	20.90	52.57	0.82	6.46	4.88	0.11	20.78	7.44	2.39	4.46	0.10	100.00	0.31	0.21
149	20.30	54.88	1.16	9.58	6.99	0.22	13.49	4.37	2.79	6.41	0.10	100.00	0.71	0.47
148	20.10	57.44	0.92	12.73	7.03	0.18	6.43	3.89	2.67	8.61	0.10	100.00	1.98	1.34
147	20.05	56.60	0.92	12.33	5.88	0.14	6.54	5.75	2.76	8.99	0.11	100.00	1.89	1.37
146	19.95	56.19	0.91	10.80	7.42	0.15	9.68	4.79	2.04	7.93	0.10	100.00	1.12	0.82

Sample ID	Depth from Bottom	Elements Present in Weight Percent: Normalized Data											Ratios	
GAL	Meters	SiO_2	TiO_2	Al_2O_3	Fe_2O_3	MnO	MgO	CaO	Na_2O	K_2O	P_2O_5	Total	Al_2O_3/ MgO	K_2O/ MgO
145-T	19.80	63.52	0.84	16.38	4.18	0.03	1.53	0.63	6.03	6.82	0.05	100.00	10.74	4.47
144	19.30													
143	19.10	52.50	0.91	10.22	6.17	0.11	10.63	10.34	2.58	6.44	0.09	100.00	0.96	0.61
142	18.95	50.60	0.94	10.34	5.91	0.18	14.26	8.98	2.05	6.60	0.14	100.00	0.72	0.46
141	18.60	46.11	0.72	8.71	4.91	0.17	14.71	16.97	1.92	5.55	0.22	100.00	0.59	0.38
140	18.30	50.99	0.84	10.38	5.59	0.17	12.40	9.85	3.02	6.67	0.09	100.00	0.84	0.54
139	18.00	57.20	0.73	9.73	5.14	0.10	12.38	6.04	2.78	5.83	0.08	100.00	0.79	0.47
137-C	17.85	48.60	0.64	7.00	4.18	0.18	12.45	20.32	2.29	4.26	0.09	100.00	0.56	0.34
136-C	17.15	34.36	0.49	5.89	2.63	0.20	8.56	42.13	1.95	3.72	0.07	100.00	0.69	0.43
135	17.10	56.24	0.84	7.50	6.95	0.09	16.71	3.56	2.87	5.17	0.07	100.00	0.45	0.31
105	16.95	49.91	0.66	9.10	4.84	0.13	9.52	16.30	3.73	5.72	0.08	100.00	0.96	0.60
104-T	16.70	54.68	0.34	13.06	4.77	0.09	3.27	12.90	4.21	6.58	0.09	100.00	4.00	2.01
103	16.50	48.92	0.82	9.68	4.91	0.15	7.08	18.94	3.10	6.24	0.16	100.00	1.37	0.88
102	16.15	55.34	1.07	10.63	5.92	0.15	9.22	6.93	3.15	7.48	0.13	100.00	1.15	0.81
101-T	16.05	45.10	0.90	7.82	4.82	0.37	8.27	25.45	1.98	5.16	0.11	100.00	0.95	0.62
99	16.00	56.54	1.09	11.39	7.13	0.19	7.43	6.14	2.62	7.36	0.12	100.00	1.53	0.99
100-T	16.00	53.05	0.99	10.12	9.00	0.20	7.55	9.52	2.14	7.29	0.15	100.00	1.34	0.97
98	15.95													
97	15.90	56.89	0.74	12.56	7.39	0.18	4.96	6.34	3.31	7.50	0.12	100.00	2.53	1.51
96	15.85	55.06	1.17	10.06	6.81	0.17	9.23	7.87	2.31	7.19	0.13	100.00	1.09	0.78
95	15.70	58.33	0.48	14.11	6.10	0.10	3.08	6.27	3.47	7.92	0.15	100.00	4.59	2.57
94	15.60	54.31	1.01	8.83	5.73	0.14	10.89	9.50	2.94	6.50	0.15	100.00	0.81	0.60
92	15.05	46.25	1.17	9.43	11.58	0.09	5.73	16.35	2.25	7.03	0.12	100.00	1.64	1.23
91	15.00	44.64	0.85	6.66	4.18	0.17	10.37	25.25	2.93	4.80	0.15	100.00	0.64	0.46
90	14.80	54.36	0.92	8.09	4.33	0.12	12.21	11.27	3.11	5.43	0.16	100.00	0.66	0.44

Sample ID	Depth from Bottom	Elements Present in Weight Percent: Normalized Data											Ratios	
GAL	Meters	SiO_2	TiO_2	Al_2O_3	Fe_2O_3	MnO	MgO	CaO	Na_2O	K_2O	P_2O_5	Total	Al_2O_3/ MgO	K_2O/ MgO
89	14.55	50.00	0.79	6.74	4.65	0.12	11.87	17.52	2.33	5.77	0.20	100.00	0.57	0.49
88	14.40	57.14	0.68	4.78	3.98	0.14	19.67	6.29	2.84	4.32	0.14	100.00	0.24	0.22
87-CN	14.30	56.24	0.67	4.62	3.72	0.10	20.27	6.96	3.14	4.10	0.16	100.00	0.23	0.20
86	14.24	46.93	0.60	4.41	3.29	0.10	15.02	22.70	3.21	3.64	0.09	100.00	0.29	0.24
85-T	14.20	50.08	0.54	12.81	9.61	0.09	5.52	10.55	3.08	7.59	0.13	100.00	2.32	1.37
84	14.15	47.85	0.76	5.93	4.37	0.09	13.73	19.98	2.76	4.38	0.14	100.00	0.43	0.32
93	14.15	54.39	1.03	7.79	5.25	0.13	12.90	9.93	2.41	5.95	0.22	100.00	0.60	0.46
83-C	14.10	41.52	0.63	4.86	3.54	0.09	11.91	30.20	3.22	3.91	0.12	100.00	0.41	0.33
82	14.05													
80-C	13.95	40.93	0.64	4.15	3.83	0.10	15.47	26.28	4.78	3.74	0.06	100.00	0.27	0.24
81	13.90	50.70	0.73	6.11	5.36	0.10	17.38	10.26	4.07	5.23	0.06	100.00	0.35	0.30
79	13.70	49.15	0.63	4.54	3.47	0.06	21.69	13.30	4.21	2.88	0.06	100.00	0.21	0.13
78	13.60	52.56	0.73	7.11	4.75	0.10	16.29	9.50	3.41	5.49	0.07	100.00	0.44	0.34
77	13.50	42.65	0.60	4.47	3.73	0.08	19.60	22.19	3.73	2.86	0.08	100.00	0.23	0.15
76	13.45	51.59	0.70	4.97	3.94	0.07	21.85	9.06	4.20	3.56	0.06	100.00	0.23	0.16
75-C	13.40	44.47	0.64	4.39	3.54	0.09	19.36	20.23	3.60	3.62	0.06	100.00	0.23	0.19
74-C	13.15	50.12	0.68	5.47	4.25	0.08	19.90	12.60	3.08	3.73	0.08	100.00	0.28	0.19
134-C	12.80	53.26	0.57	4.85	4.01	0.06	20.08	10.66	2.93	3.50	0.09	100.00	0.24	0.17
133-D	12.30	26.44	0.63	4.56	3.69	0.23	30.18	29.00	1.96	3.12	0.18	100.00	0.15	0.10
132-D	12.05	36.04	0.74	5.53	4.06	0.18	26.69	20.47	2.15	4.03	0.11	100.00	0.21	0.15
131	11.95													
130	11.85	53.68	0.93	6.92	4.55	0.10	16.13	10.00	2.91	4.68	0.10	100.00	0.43	0.29
129	11.70	52.30	0.98	8.50	6.50	0.16	9.30	12.37	2.88	6.88	0.12	100.00	0.91	0.74
128	11.30	50.33	0.79	11.12	13.63	0.09	4.26	8.52	3.60	7.47	0.20	100.00	2.61	1.75
127	11.15	56.92	1.37	10.07	6.90	0.10	10.81	2.10	3.54	8.10	0.10	100.00	0.93	0.75

Sample ID	Depth from Bottom	Elements Present in Weight Percent: Normalized Data											Ratios	
GAL	Meters	SiO_2	TiO_2	Al_2O_3	Fe_2O_3	MnO	MgO	CaO	Na_2O	K_2O	P_2O_5	Total	Al_2O_3/ MgO	K_2O/ MgO
126	11.05	53.56	0.89	11.64	8.59	0.12	5.45	7.49	3.34	8.72	0.21	100.00	2.14	1.60
125	10.95	54.81	0.91	7.03	4.92	0.08	14.59	8.25	4.06	5.25	0.11	100.00	0.48	0.36
124-T	10.90	27.68	0.42	3.85	12.85	0.07	4.86	44.40	2.92	2.85	0.10	100.00	0.79	0.59
123	10.80	51.62	0.88	6.76	4.95	0.10	13.99	10.95	5.34	5.30	0.11	100.00	0.48	0.38
122-C	10.30	53.32	0.90	6.96	5.13	0.09	14.18	10.30	3.84	5.18	0.11	100.00	0.49	0.37
121	10.05	56.32	1.02	7.81	5.52	0.08	13.68	6.50	3.31	5.67	0.09	100.00	0.57	0.41
120	9.95	50.63	1.01	8.51	5.87	0.11	9.20	14.25	4.12	6.09	0.20	100.00	0.92	0.66
119	9.70	51.60	0.82	6.79	5.08	0.09	13.79	12.98	3.42	5.29	0.13	100.00	0.49	0.38
118	9.55	52.10	0.88	6.82	4.92	0.11	14.18	12.14	3.49	5.21	0.14	100.00	0.48	0.37
117-T	9.45	49.39	1.04	8.54	7.68	0.12	8.50	15.22	3.28	6.05	0.19	100.00	1.00	0.71
116	9.10	55.14	1.14	8.56	6.37	0.08	12.54	5.89	3.57	6.56	0.16	100.00	0.68	0.52
115	9.00	49.90	0.87	6.25	4.61	0.11	15.02	14.23	4.49	4.44	0.09	100.00	0.42	0.30
114	8.90	50.71	0.70	5.85	4.53	0.09	17.27	11.99	4.76	4.00	0.10	100.00	0.34	0.23
113-T	8.80	45.04	0.58	4.51	3.62	0.17	22.66	13.75	6.53	3.05	0.08	100.00	0.20	0.13
112	8.50	49.48	0.71	5.54	4.16	0.09	19.00	10.81	6.13	4.00	0.07	100.00	0.29	0.21
111	8.30	45.94	0.74	5.72	3.97	0.10	23.93	11.59	3.95	3.97	0.09	100.00	0.24	0.17
110	8.10	54.66	0.89	6.71	4.71	0.08	20.59	3.34	4.42	4.51	0.09	100.00	0.33	0.22
109	8.00	36.44	0.76	5.94	4.83	0.11	21.71	16.71	9.44	3.98	0.08	100.00	0.27	0.18
108	7.85													
107	7.55	40.13	0.83	6.14	4.37	0.10	25.31	14.60	3.95	4.52	0.06	100.00	0.24	0.18
106	7.40	41.02	0.81	6.01	4.42	0.10	24.73	14.17	4.15	4.51	0.07	100.00	0.24	0.18
35	7.00	44.78	0.86	6.53	4.37	0.10	23.43	12.17	3.14	4.53	0.09	100.00	0.28	0.19
34	6.90	34.37	0.62	4.47	3.70	0.08	29.00	21.89	2.56	3.26	0.05	100.00	0.15	0.11
33	6.60	37.67	0.65	4.73	3.63	0.08	28.91	19.26	1.71	3.29	0.07	100.00	0.16	0.11
32	6.30	26.36	0.46	3.90	3.43	0.11	30.61	28.05	4.08	2.80	0.20	100.00	0.13	0.09

Sample ID	Depth from Bottom	Elements Present in Weight Percent: Normalized Data											Ratios	
GAL	Meters	SiO_2	TiO_2	Al_2O_3	Fe_2O_3	MnO	MgO	CaO	Na_2O	K_2O	P_2O_5	Total	Al_2O_3/ MgO	K_2O/ MgO
31	6.05	50.77	0.75	6.05	4.61	0.07	24.11	4.68	4.96	3.92	0.08	100.00	0.25	0.16
30-C	6.00	44.62	0.80	6.33	4.55	0.08	15.74	17.48	5.87	4.43	0.08	100.00	0.40	0.28
29-C	5.80	37.14	0.74	5.87	4.56	0.09	13.14	29.91	4.14	4.33	0.08	100.00	0.45	0.33
28-C	5.60	48.08	0.91	7.16	5.21	0.08	14.32	13.43	5.67	5.07	0.08	100.00	0.50	0.35
27	5.40	42.51	0.92	7.06	4.84	0.09	15.71	17.82	5.74	5.23	0.08	100.00	0.45	0.33
26	5.05	35.46	0.84	6.29	4.71	0.11	23.15	19.51	4.72	5.12	0.09	100.00	0.27	0.22
25	5.00	44.61	0.60	12.50	11.70	0.04	5.06	11.81	6.75	6.78	0.16	100.00	2.47	1.34
24-T	4.95	32.55	0.58	3.73	2.82	0.10	29.81	22.48	5.00	2.85	0.08	100.00	0.13	0.10
23	4.60	41.15	0.65	4.96	3.51	0.10	26.40	15.21	4.10	3.81	0.10	100.00	0.19	0.14
22	4.20	41.92	0.69	4.13	3.22	0.11	27.70	15.61	3.49	3.03	0.11	100.00	0.15	0.11
21	4.10	41.83	0.38	2.93	2.32	0.05	18.44	27.80	4.07	2.13	0.05	100.00	0.16	0.12
20	4.00	39.43	0.62	6.27	4.37	0.08	10.08	27.56	6.38	5.13	0.08	100.00	0.62	0.51
19-T	3.80	46.57	1.06	8.53	6.49	0.09	10.99	18.82	2.83	4.45	0.18	100.00	0.78	0.41
18-T	3.60	44.97	0.93	9.61	7.22	0.15	16.05	12.57	5.58	2.84	0.06	100.00	0.60	0.18
17-T	3.40	45.55	1.41	9.95	7.39	0.14	12.01	15.99	4.12	3.35	0.09	100.00	0.83	0.28
16-T	3.20	41.61	0.96	9.49	6.90	0.15	10.07	23.70	3.26	3.69	0.20	100.00	0.94	0.37
15	3.00	51.27	1.18	6.87	4.69	0.12	17.60	11.79	3.01	3.35	0.13	100.00	0.39	0.19
14	2.80	50.22	1.10	6.83	4.98	0.22	17.42	12.62	3.35	3.15	0.12	100.00	0.39	0.18
13	2.60	56.72	1.12	8.97	5.48	0.08	16.43	3.49	3.80	3.78	0.13	100.00	0.55	0.23
12	2.40	51.87	0.86	5.95	4.59	0.13	19.43	10.69	3.47	2.89	0.13	100.00	0.31	0.15
11	2.20	49.98	0.93	7.47	4.88	0.10	16.85	12.22	4.27	3.19	0.11	100.00	0.44	0.19
10	2.00	57.56	1.49	11.32	7.80	0.18	9.34	3.80	2.62	5.74	0.14	100.00	1.21	0.61
9	1.80	55.08	1.48	12.40	7.89	0.29	3.80	9.28	3.51	5.91	0.36	100.00	3.26	1.55
8	1.60	57.66	1.53	13.24	9.89	0.36	5.50	1.82	2.36	7.22	0.43	100.00	2.41	1.31
7	1.40	57.36	1.48	12.78	9.63	0.78	5.42	2.86	2.56	6.58	0.54	100.00	2.36	1.21

Sample ID	Depth from Bottom	Elements Present in Weight Percent: Normalized Data											Ratios	
GAL	Meters	SiO_2	TiO_2	Al_2O_3	Fe_2O_3	MnO	MgO	CaO	Na_2O	K_2O	P_2O_5	Total	Al_2O_3/ MgO	K_2O/ MgO
6	1.20	51.75	1.35	12.04	9.35	1.55	4.43	9.31	3.12	6.38	0.72	100.00	2.72	1.44
5-T	1.00	56.46	1.33	13.10	8.78	0.30	3.53	5.46	5.02	5.72	0.30	100.00	3.71	1.62
4-T	0.75	57.13	1.36	13.42	8.07	0.12	3.46	4.85	5.81	5.53	0.26	100.00	3.88	1.60
3-T	0.50	50.95	1.18	12.25	7.48	0.51	2.51	14.52	5.57	4.60	0.44	100.00	4.88	1.83
2-T	0.25	59.97	1.19	14.46	7.65	0.08	2.04	1.90	7.19	5.23	0.28	100.00	7.07	2.56
1-T	0.00	60.13	1.37	14.40	8.45	0.09	1.85	1.95	6.44	4.99	0.33	100.00	7.77	2.69

Appendix C: Error Estimates for XRF Major Element Oxide and Trace Elements Data

Variations in United States Geological Survey (USGS) Standard Reference Material BHV01 preceding XRF major element oxide and trace element analysis.

Sample BHVO1	Elements by Weight Percent										Total	Elements Present in PPM				
Date	SiO_2	TiO_2	Al_2O_3	Fe_2O_3	MnO	MgO	CaO	Na_2O	K_2O	P_2O_5	%	Rb	Sr	Y	Zr	Nb
Publish	49.94	2.71	13.80	12.23	0.17	7.23	11.40	2.26	0.52	0.27	100.53	11	403	28	179	19
1/28/2010	50.92	2.84	14.90	12.30	0.19	8.80	11.23	3.51	0.68	0.35	105.72	10	374	30	150	14
1/29/2010	52.96	2.88	14.97	12.38	0.19	8.98	11.37	3.75	0.71	0.36	108.55	15	368	25	150	11
2/1/2010	53.21	2.95	15.04	12.52	0.20	9.27	11.43	3.86	0.72	0.37	109.57	9	368	30	151	15
2/2/2010	53.25	2.95	15.04	12.57	0.19	9.18	11.37	3.82	0.71	0.37	109.45	10	374	29	149	16
2/3/2010	53.58	2.95	15.00	12.08	0.19	9.27	11.07	3.79	0.69	0.37	108.99	9	371	30	150	15
2/3/2010	52.88	2.94	15.00	12.24	0.19	9.19	11.17	3.81	0.68	0.37	108.47	9	367	26	150	15
2/3/2010	52.96	2.93	15.09	12.31	0.19	9.11	11.24	3.75	0.69	0.37	108.64					
2/4/2010	52.78	2.90	14.81	12.05	0.19	8.99	11.06	3.75	0.70	0.38	107.61	14	370	29	152	17
2/10/2010	53.58	3.02	15.11	12.44	0.19	9.46	11.30	3.98	0.71	0.38	110.17	12	371	29	146	14
2/15/2010	53.68	3.02	15.15	12.51	0.19	9.55	11.30	4.00	0.72	0.38	110.50	10	371	28	148	14
2/16/2010	52.75	2.98	15.02	12.27	0.19	9.37	11.08	3.87	0.69	0.38	108.60	10	375	26	147	12
2/17/2010	53.55	2.98	14.92	12.28	0.19	9.34	11.13	3.95	0.71	0.38	109.43	10	372	24	151	16
3/1/2010	53.48	2.90	14.86	11.74	0.19	9.25	10.71	3.90	0.68	0.38	108.09	10	372	32	150	13
3/3/2010	53.58	2.91	14.83	11.98	0.19	9.16	10.92	3.92	0.69	0.39	108.57	17	372	28	149	14
3/15/2010	53.54	2.83	14.89	11.40	0.19	9.32	10.45	3.80	0.66	0.39	107.47	15	372	22	151	15
3/17/2010	53.16	2.83	14.54	11.47	0.18	8.90	10.61	3.73	0.68	0.39	106.49	13	376	28	149	16
3/22/2010	53.44	2.88	14.72	11.54	0.18	9.07	10.70	3.88	0.68	0.39	107.48	11	371	24	148	17
3/24/2010	52.94	2.83	14.65	11.50	0.18	8.82	10.58	3.74	0.67	0.39	106.30	9	373	29	147	15
4/14/2010	52.85	2.73	14.37	11.04	0.18	8.50	10.33	3.72	0.65	0.39	104.76	11	370	27	150	14
4/21/2010	54.57	3.16	15.32	12.81	0.19	10.13	11.48	4.22	0.71	0.40	112.99	12	371	25	152	12
4/28/2010	54.62	3.16	15.29	12.77	0.20	10.15	11.50	4.22	0.72	0.40	113.03	10	376	28	149	17

Sample BHVO1	Elements by Weight Percent										Total	Elements Present in PPM				
Date	SiO_2	TiO_2	Al_2O_3	Fe_2O_3	MnO	MgO	CaO	Na_2O	K_2O	P_2O_5	%	Rb	Sr	Y	Zr	Nb
6/13/2010	51.16	2.80	14.67	11.98	0.19	8.51	11.02	3.81	0.67	0.39	105.20	12	370	27	149	14
MEAN	53.16	2.93	14.92	12.10	0.19	9.20	11.05	3.85	0.69	0.38		11.33	371.62	27.43	149.43	14.57
ST DEV	0.85	0.10	0.23	0.47	0.01	0.41	0.35	0.16	0.02	0.01		2.29	2.46	2.46	1.60	1.66
"+/-%"	1.59	3.58	1.55	3.92	2.78	4.45	3.12	4.13	2.91	3.29		20.19	0.66	8.97	1.07	11.40

Appendix D: Trace Element Data from XRF analysis

*Sample lithology is claystone unless otherwise noted: CN=chert nodules in claystone, T=tuff/inclusion of tuff, D=dolostone/dolomite, C=presence of calcite

Sample ID	Depth from Bottom	Trace Elements Present in PPM				
GAL	Meters	Rb	Sr	Y	Zr	Nb
179	34.05	60	696	16	133	25
178	33.40	49	1256	28	148	20
177	32.90	100	488	23	277	76
176	32.00	99	628	22	256	62
174-T	31.90	67	794	17	171	32
175	31.70	104	370	21	276	70
173	31.30	93	795	31	249	55
172	31.00	77	1675	34	260	43
171	30.20	41	990	22	139	25
170	30.10	28	1010	18	100	16
169	30.05	70	1317	27	211	34
168	29.95	109	1370	39	274	54
166	29.85	123	653	20	302	67
165	29.55	137	1171	27	293	61
167	29.50					
164	29.40	136	1385	22	266	60
163-C	29.20	61	1469	12	187	33
162	29.15	112	1084	33	233	53
161	29.10	97	684	25	188	46
160	29.00	98	526	36	208	56
159	28.80	66	460	28	167	43
158	28.70					
157-C	28.20	60	749	31	163	38
156	28.10	154	129	8	296	68
155	27.95					
154-C	27.55	88	340	14	172	51
153	27.50	66	462	12	317	103
152	27.20					
151	27.10	101	254	12	332	104
36-D	27.05	131	10626	4	663	60
37	27.00	101	1324	29	217	52
38	26.80	120	894	26	242	59
39	26.75	70	1062	26	185	41

Sample ID	Depth from Bottom	Trace Elements Present in PPM				
GAL	Meters	Rb	Sr	Y	Zr	Nb
40	26.70	58	1287	47	164	29
41	26.35					
42	26.15	99	1604	49	221	51
43	26.05	130	759	31	262	72
44	25.95	125	611	36	268	74
45	25.85	94	493	33	209	57
46	25.70	120	475	18	194	61
47	25.60	113	506	25	200	62
48	25.20	140	509	25	263	67
49	25.05	122	573	15	336	68
50	24.95	78	226	8	212	41
51	24.70	122	437	11	370	77
52-T	24.55	65	818	22	275	77
53-T	24.40	106	423	41	489	105
54-T	24.30	69	582	6	281	70
55-T	24.20	101	357	34	334	80
56	24.10	102	591	39	317	75
57-T	24.05	93	471	23	356	82
58	23.95	112	452	29	214	81
59	23.90	132	380	17	200	71
60	23.80	131	536	23	245	70
61-T	23.50	140	3743	7	474	81
62	23.30	114	260	20	248	69
63	23.05	146	328	34	245	79
64-T	22.80	111	419	31	285	74
65	22.60	141	354	22	361	86
66	22.50	135	263	20	366	90
68	21.80	117	689	29	241	67
67-T	21.73	76	317	6	351	78
69	21.70	121	525	23	259	68
70	21.40	132	446	23	248	74
71	21.00	132	430	25	259	77
72	20.95	90	1464	16	154	27
73	20.90	138	650	6	134	39
149	20.30	163	230	35	242	92
148	20.10	127	285	27	350	90
147	20.05	139	336	22	439	101

Sample ID	Depth from Bottom	Trace Elements Present in PPM				
GAL	Meters	Rb	Sr	Y	Zr	Nb
146	19.95	135	178	29	357	82
145-T	19.80	79	220	13	441	91
144	19.30					
143	19.10	140	275	29	236	74
142	18.95	142	499	20	264	78
141	18.60	105	723	31	221	79
140	18.30	145	415	22	267	90
139	18.00	121	278	17	212	77
137-C	17.85	92	498	47	180	58
136-C	17.15	67	733	50	154	34
135	17.10	148	90	2	215	79
105	16.95	115	363	16	264	64
104-T	16.70	67	363	18	312	49
103	16.50	93	700	45	298	60
102	16.15	132	366	27	361	73
101-C	16.05	92	719	42	238	48
99	16.00	129	354	29	331	81
100-T	16.00	111	882	39	298	61
98	15.95					
97	15.90	111	495	21	286	62
96	15.85	131	396	31	285	72
95	15.70	86	571	17	275	64
94	15.60	124	585	32	282	69
92	15.05	100	6456	-2	472	32
91	15.00	91	1478	25	205	44
90	14.80	122	1268	16	229	53
89	14.55	91	1479	23	186	46
88	14.40	112	646	9	168	52
87-CN	14.30	112	488	10	154	51
86	14.24					
85	14.20	73	1377	8	165	29
84	14.15	90	1407	17	193	34
93	14.15	120	877	31	280	65
83-C	14.10	70	1155	16	156	27
82	14.05					
80-C	13.95	77	1151	4	132	21
81	13.90	128	329	7	93	27

Sample ID	Depth from Bottom	Trace Elements Present in PPM				
GAL	Meters	Rb	Sr	Y	Zr	Nb
79	13.70	88	603	12	88	28
78	13.60	113	385	0	94	27
77	13.50	89	1057	13	107	28
76	13.45	110	492	8	84	32
75-C	13.40	103	808	16	99	19
74-C	13.15	114	788	22	123	35
134-C	12.80	116	379	7	76	30
133-D	12.30	85	2279	5	178	33
132-D	12.05	100	1919	7	176	26
131	11.95					
130	11.85	114	328	15	159	37
129	11.70	134	452	18	274	46
128	11.30	87	724	9	177	31
127	11.15	168	123	13	251	61
126	11.05	116	516	18	191	39
125	10.95	127	386	18	184	37
124-T	10.90	46	1301	26	120	10
123	10.80	113	449	19	173	32
122-C	10.30	117	557	18	191	41
121	10.05	134	348	17	212	44
120	9.95	120	487	5	90	31
119	9.70	109	676	20	186	35
118	9.55	109	748	19	189	31
117	9.45	87	455	13	148	28
116	9.10	150	471	7	226	44
115	9.00	119	1092	7	172	30
114	8.90	114	1511	9	166	31
113-T	8.80	100	1353	4	128	22
112	8.50	116	974	5	123	28
111	8.30	116	973	3	123	27
110	8.10	151	243	8	110	39
109	8.00	104	1038	-2	118	23
108	7.85					
107	7.55	138	1026	0	143	33
106	7.40	129	1063	4	146	27
35	7.00	141	807	11	148	31
34	6.90	97	1517	-1	145	22

Sample ID	Depth from Bottom	Trace Elements Present in PPM				
GAL	Meters	Rb	Sr	Y	Zr	Nb
33	6.60	106	1510	5	150	23
32	6.30	77	1630	14	130	15
31	6.05	161	440	8	115	37
30-C	6.00	129	1164	12	143	30
29-C	5.80	105	1412	19	147	23
28-C	5.60	155	881	7	152	31
27	5.40	137	849	4	148	32
26	5.05	113	1678	10	191	27
25	5.00	61	1876	-4	164	17
24-T	4.95	68	1356	7	136	20
23	4.60	64	1089	17	149	23
22	4.20	77	1086	4	146	29
21	4.10	45	719	13	82	14
20	4.00	63	1346	7	153	22
19-T	3.80	66	1357	12	161	32
18-T	3.60	46	825	7	95	15
17-T	3.40	73	742	8	119	32
16-T	3.20	54	1366	15	154	23
15	3.00	108	849	18	181	45
14	2.80	88	787	10	178	41
13	2.60	109	437	8	207	53
12	2.40	97	755	8	175	35
11	2.20	79	777	17	202	36
10	2.00	202	306	11	321	84
9	1.80	167	638	44	354	70
8	1.60	230	222	51	416	88
7	1.40	231	334	48	378	85
6	1.20	197	591	55	342	68
5-T	1.00	153	371	71	461	95
4-T	0.75	137	397	71	455	99
3-T	0.50	117	997	124	417	78
2-T	0.25	125	350	71	455	99
1-T	0.00	119	354	87	492	113